REMARKS

Applicants respectfully requests reconsideration of the present application in view of the foregoing amendments and the following reasons.

I. Status of the Claims

Claims 3, 23, 24, 37, 41, 45, and 49 were cancelled previously. Claims 1, 30 and 35 have been amended to more clearly set forth the claimed subject matter and to recite that the drug particles are in a crystalline phase, an amorphous phase, or a mixture thereof, with exemplary support in the original claims and original specification, e.g., at page 5, first full paragraph; and at page 6, lines 13-15.

Applicants acknowledge the finality of the outstanding Office Action. However, the claim amendments: (i) do not introduce any new matter; (ii) rephrase the claimed subject matter for greater clarity; (iii) do not require any additional search; and (iv) place the application in condition for allowance or at least in better condition for appeal. Accordingly, Applicants respectfully request entry of this amendment. Upon entry, claims 1-2, 4-22, 25-36, 38-40, 42-44, 46-48, and 50-54 are pending.

II. Rejection of Claims under 35 U.S.C. §102(b)

Claims 1, 2, 4, 8-13, 30-36, 38-40, 46-48 and 50-54 are rejected under 35 U.S.C. §102(b) for alleged anticipation by PCT Publication No. WO 96/20698 by Levy et al. ("Levy"). Applicants respectfully traverse the rejection.

A. Levy does not teach a surface stabilizer associated with the surface of drug particles, as required by the claimed invention

As submitted in the response filed on November 8, 2010, the teachings of Levy fail to meet the claim limitation of a surface stabilizer associated with the surface of the nanoparticulate drug particles. *See* pages 16-17.

In reply, the Examiner misinterprets the teaching of Levy in an attempt to meet the claim limitations. Specifically, in the final Office Action, the Examiner contends that the "surface modifying agent" of Levy's composition teaches or suggests the surface stabilizer of the claimed invention by making reference to Levy at pages 12-15, and at page 20, lines 11-20. *See* final Office Action, page 2, lines 10-12. A number of surface modifying agents are exemplified at pages 13-15 of Levy. At page 20, Levy elaborates that the surface modifying agent may be adsorbed on "the surface of pre-formed nanoparticles" rather than on the surface of the drug particles as prescribed by the claimed invention. Levy, page 20, lines 13-15. As Levy clearly describes, the drug is "incorporated, embedded, entrained, or otherwise made part of the polymer matrix" to form the nanoparticles. Levy, page 7, 1st paragraph. Accordingly, Levy's "particles" *do not* consist solely of a drug, which is the case in Applicants' claimed invention. Rather, the composition of Levy has a structure as depicted in Figure 1 below, wherein drug particle are encapsulated within a PLGA nanoparticle. This structure prevents the surface modifying agent of Levy from direct adsorption onto the surface of the drug particles. In the composition of Levy, the surface modifying agent can *only* adsorb on the surface of the PLGA nanoparticles, in which the drug particles are embedded.

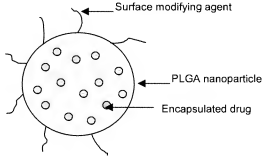

Figure 1

See also, Banerjee et al., "Nanotechnology-mediated targeting of tumor angiogenesis," *Vascular Cell*, 3:3 (2011) (Exhibit A), Figure 1, for the structure of an exemplary PLGA nanoparticle.

In sharp contrast, the structure of Applicants' claimed nanoparticulate drug composition has at least one surface stabilizer is *directly* associated with the surface of the drug particles, as shown in Figure 2 below:

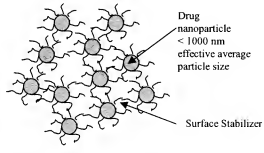

Figure 2

B. The intermediate product of Levy does not teach the claimed invention having a surface stabilizer directly associated with the surface of drug nanoparticles

The Examiner insists that Levy's teachings meet the claim limitation of a surface stabilizer associated with the surface of the active agent particles. According to the Examiner, Examples 1 and 2 of Levy disclose that the active agent "came in direct contact with the surface stabilizer solution." Final Office Action, page 4, 1st full paragraph. Applicants respectfully submit that the Examiner's interpretation of Levy's teaching is incorrect.

The Examiner arbitrarily takes the teaching of Levy out of context. In Examples 1 and 2, Levy describes that the polymer and drug are co-dissolved in an organic solvent, added to an aqueous PVA solution to form an emulsion, and then the solvent is evaporated and the nanoparticles are washed and recovered. *See* page 31. Although the Examiner does not explicitly state which ingredients of Levy's composition teach or suggest which ingredients of the claimed invention, presumably the Examiner is alleging that the polymer of Levy's composition allegedly teaches or suggests the polymer matrix of the claimed invention, and the

PVA solution of Levy's composition allegedly teaches or suggests the surface stabilizer of the claimed invention.

In the intermediate product of the oil-in-water emulsion of Levy, the Examiner asserts that the surface stabilizer solution (the PVA solution) "came in direct contact" with the active agent, which is also dissolved in an organic solvent along with the polymer. In other words, in the emulsion phase, the surface stabilizer solution is in direct contact with the active agent, which allegedly meets Applicants' claim limitation of a surface stabilizer associated with the surface of the active agent particle. This allegation is incorrect, because in the emulsion of Levy, the active agent is *completely dissolved in the organic solvent and NOT in a particulate form.* Therefore, the active agent has no surface for the surface stabilizer to be associated with.

C. The PVA is removed from Levy's final product and, therefore, Levy fails to teach Applicants' claimed invention requiring a surface stabilizer associated with nanoparticulate drug particles

Moreover, Levy further describes that the nanoparticles are washed during recovery. This step would have removed the PVA, which is soluble in water. *See* page 31, lines 8-11, which describes that PVA was pre-filtered to ensure that high molecular weight PVA molecules are removed and that the remaining PVA molecules are water-soluble. The fact that PVA is *removed* from the final product of nanoparticles is further evidenced by Desai et al., "Gastrointestinal uptake of biodegradable microparticles: effect of particle size," *Pharmaceutical Research*, *13*(12): 1838-1845 (1996) (Exhibit B). Both Exhibit B and the cited reference have the common inventors/authors of Robert Levy and Vinod Labhasetwar. Both describe the formulation of PLGA nanoparticles. In Exhibit B, BSA was used as an exemplary drug to form PLGA nanoparticles. Exhibit B explicitly discloses that PVA is *removed* by washing the nanoparticles during recovery. *See* page 1839, left column, lines 13-15.

In view of the foregoing, the Examiner has no valid basis to rely on Examples 1 and 2 of Levy for the alleged teaching of a surface stabilizer associated with the surface of drug particles.

This is because when the surface stabilizer solution (PVA solution) is in contact with the active agent, the active agent is in a dissolved form and provides no surface for the surface stabilizer to be associated with. Furthermore, when the final product of the nanoparticles are recovered, Levy teaches a step of removing PVA from the PLGA nanoparticles.

D. Levy fails to teach a composition having discrete drug particles in a crystalline phase, an amorphous phase, or a mixture thereof, as prescribed by the claimed invention.

The emulsion process of Levy does not yield discrete drug particles in a crystalline phase, an amorphous phase, or a mixture thereof. Rather, the polymeric particles of Levy in which the drug substance is "incorporated, embedded, entrained or otherwise made part of the polymer matrix" (page 7, lines 1-4). In Levy's process, the drug must first be dissolved (i.e. dispersed at ***molecular level***) in a solvent material which is later evaporated: "[e]vaporation of the organic solvent solidifies the liquid droplets into small solid particles, termed the 'polymeric core' . . . . Bioactive agent dissolved in either an aqueous or organic phase becomes part of the polymeric core matrix" (page 30, lines 10-12). From the description of Levy's emulsion process, it appears that the molecularly dispersed nature of the drug is maintained in the polymeric cores. In other words, the drug particles of Levy's composition are a molecular dispersion of the drug throughout a polymeric carrier matrix. Apart from the above passage from page 7, Levy is silent as to the precise form of the drug in the final composition, let alone any explicit disclosure that the drug particles are in a crystalline phase, an amorphous phase, or a mixture thereof to meet the claim limitations. Moreover, because Levy teaches molecularly dispersed drug, the skilled artisan would understand that Levy's composition has no drug particle surface to which to associate a surface stabilizer.

Accordingly, withdrawal of the rejection is warranted because the cited reference fails to teach or suggest each and every aspect of the claimed invention.

III. Rejection of Claims under 35 U.S.C. §103(a)

Claims 1, 2, 4-22, 25-36, 38-40, 42-44, 46-48, and 50-54 are rejected under 35 U.S.C. §103(a) for allegedly being obvious over Levy in view of PCT Publication No. WO 99/02665 by Liversidge et al. ("Liversidge"). Applicants respectfully traverse the rejection.

The teachings of Levy are discussed *supra*. The Examiner cites Liversidge for the alleged teaching of tablets comprising nanoparticles and pharmaceutically acceptable excipients. *See* final Office Action, page 3, 1st and 2nd paragraphs. However, Liversidge is not cited for any compensation for the deficiencies of Levy, which fails to meet the structural limitations of the claimed invention as detailed above. Therefore, the claimed invention is nonobvious in view of the combined teachings of Levy and Liversidge. Accordingly, Applicants respectfully request withdrawal of the rejection.

CONCLUSION

The present application is now in condition for allowance. Favorable reconsideration of the application as amended is respectfully requested. The Examiner is invited to contact the undersigned by telephone if it is felt that a telephone interview would advance the prosecution of the present application.

The Commissioner is hereby authorized to charge any additional fees which may be required regarding this application under 37 C.F.R. §§ 1.16-1.17, or credit any overpayment, to Deposit Account No. 19-0741. Should no proper payment be enclosed herewith, as by the credit card payment instructions in EFS-Web being incorrect or absent, resulting in a rejected or incorrect credit card transaction, the Commissioner is authorized to charge the unpaid amount to Deposit Account No. 19-0741.

If any extensions of time are needed for timely acceptance of papers submitted herewith, Applicants hereby petition for such extension under 37 C.F.R. §1.136 and authorizes payment of any such extensions fees to Deposit Account No. 19-0741.

Respectfully submitted,

Date: June 10, 2011

By 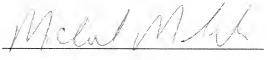

FOLEY & LARDNER LLP
Customer Number: 31049
Telephone: (202) 672-5538
Facsimile: (202) 672-5399

Michele M. Simkin
Attorney for Applicant
Registration No. 34,717

EXHIBIT A

VASCULAR CELL

REVIEW Open Access

Nanotechnology-mediated targeting of tumor angiogenesis

Deboshri Banerjee, Rania Harfouche, Shiladitya Sengupta*

Abstract

Angiogenesis is disregulated in many diseased states, most notably in cancer. An emerging strategy for the development of therapies targeting tumor-associated angiogenesis is to harness the potential of nanotechnology to improve the pharmacology of chemotherapeutics, including anti-angiogenic agents. Nanoparticles confer several advantages over that of free drugs, including their capability to carry high payloads of therapeutic agents, confer increased half-life and reduced toxicity to the drugs, and provide means for selective targeting of the tumor tissue and vasculature. The plethora of nanovectors available, in addition to the various methods available to combine them with anti-angiogenic drugs, allows researchers to fine-tune the pharmacological profile of the drugs *ad infinitum*. Use of nanovectors has also opened up novel avenues for non-invasive imaging of tumor angiogenesis. Herein, we review the types of nanovector and therapeutic/diagnostic agent combinations used in targeting tumor angiogenesis.

Introduction

Since Judah Folkman emphasized the 'angiogenic switch' hypothesis for tumor progression in 1991, there has been a tremendous surge in targeting angiogenesis for cancer therapeutics [1]. In the past 30 years, many advances have been made in the field, with the elucidation of various angiogenic molecules that could be targeted to halt angiogenesis, and hence, tumor progression. Angiogenesis, the formation of new capillaries from preexisting vessels, is crucial for ensuring normal embryonic vascular development of all vertebrates, as well as regulating physiological processes such as menses and wound healing in adults [2-4]. Deregulation of angiogenesis hence underlies pathologies characterized by vessel overgrowth (e.g. cancer) as well as vessel insufficiency (e.g. cardiovascular disease, CVD) [4].

It is now well-established that without angiogenesis, tumors cannot grow more than 2 mm in diameter [5-7]. Studies in breast cancer patients have showed that angiogenesis positively correlates with the degree of metastasis, tumor recurrence and shorter survival rates, thus demonstrating the value of angiogenesis as a prognostic cancer marker [1,8]. Tumor angiogenesis essentially entails the same sequences of events as physiological angiogenesis, however, the latter proceeds in an uncontrolled and excessive manner giving rise to leaky and tortuous vessels that are in a constant state of inflammation [6,9]. This is mainly due by an upregulation of angiogenic cytokines and growth factors, most notably the vascular endothelial cell growth factor (VEGF) and Angiopoietin (Ang) families, as well as integrins [10-12]. Integrin $\alpha_v\beta_3$ is the best-characterized heterodimer that is upregulated in most cancer settings, both on the vasculature and on the tumor cells themselves [13,14]. It is hence not surprising that these molecules are often targeted in both experimental and clinical cancer settings.

As such, the first U.S. Food and Drug Administration (FDA) approved anti-angiogenic therapy was the monoclonal antibody Bevacizumab (Avastin), that targets VEGF proteins overexpressed on colorectal cancer cells and their vasculature [15,16]. In spite of the clinical success of Avastin, the majority of other such anti-angiogenic therapeutic agents have yet to pass phase II clinical trials, suggesting a new paradigm is essential to target aberrant angiogenesis.

Moving away from conventional chemotherapy

Targeting aberrant angiogenesis for cancer therapy

Development of anti-angiogenesis therapy is based on either drugs that prevent the formation of new blood

* Correspondence: shiladit@mit.edu
BWH-MIT Center for Biomedical Engineering, Department of Medicine, Brigham and Women's Hospital, Harvard Medical School, Harvard-MIT Division of Health Science and Technology, Cambridge, MA 02139, USA

vessels supplying to the tumor (e.g. TNP-470, endostatin, angiostatin), or drugs that damage existing blood vessels (e.g. combretastatin) [17]. The underlying mechanisms of action of these anti-angiogenic drugs are either direct, by targeting endothelial receptors, or indirect, by targeting angiogenic cytokines. These mechanisms of action differ from those of conventional chemotherapy in the following ways: (i) selective targeting of the tumor-associated vasculature instead of the tumor cells themselves; (ii) increased bioavailability of tumor endothelial cells to systemically-administered anti-angiogenic drugs due to their direct contact with blood circulation, whereas tumor cells residing in the distant tumor tissue are less accessible to conventional chemotherapeutic agents; (iii) whereas conventional chemotherapy uses the principle of maximum tolerated dose (MTD), anti-angiogenic therapy is administered in lower doses at a relatively more frequent schedule (metronomic chemotherapy), leading to significantly less systemic toxicity [18,19].

Despite these advantages of anti-angiogenic therapy over conventional chemotherapeutic methods, it still suffers from certain limitations. For instance, as a result of systemic administration, most angiogenic inhibitors often fail to reach the targeted tumor vessels, thus exhibiting a poor biodistribution and pharmacokinetic profile, with associated side effects and low efficacy. A great advance towards this end has come from harnessing the advantages of nanotechnology to more efficiently target and kill tumor-associated vasculature. These advantages are made possible by several parameters, including the size of these nanoparticles that allows them to intrinsically home in to metastasized tumors through the enhanced permeability and retention effect (EPR), their ability to evade the immune system and improve the drug's half-life significantly thus lowering its effective dose 50 (ED_{50}), and allow for potent selective targeting due to their high surface density [15,18,20,21]. For these reasons, nanotherapeutics are emerging as the new paradigm for anti-angiogenesis research.

Nanoparticle-mediated anti-angiogenesis therapy for cancer

Nanotechnology in cancer therapy includes an arsenal of nano-sized materials, generally ranging in dimensions from 1 nm to a few hundred nanometers in at least one dimension [22]. These nanoparticles are designed to carry therapeutic drugs and imaging agents, which are loaded on or within the nanocarriers by chemical conjugation or simply by encapsulation. Nanoparticle based chemotherapeutic agents are designed such that they can passively or actively target cancer cells.

The leaky vasculature associated with tumors contributes towards the phenomenon of passive targeting by nanoparticles. The tumor vessels have increased permeability due to aberrant angiogenesis, thus allowing nanoparticles with diameters less than 200 nm to passively extravasate into the tumor sites through the EPR effect. These nanoparticles are subsequently cleared by the liver [15,23]. Although many factors, including surface area and chemical modifications, can affect the nanoparticle biodistribution, size remains the limiting factor in achieving passive targeting to tumor sites. As such, nanoparticles with sizes less than 10 nm are cleared by the kidney, whereas those larger than 200 nm often accumulate in the extracellular space, and fail to reach the cancer environment *(20)*. Furthermore, poor lymphatic drainage mechanisms in tumors allow the nanoparticles to be retained in the vicinity of the tumor cells and allow them to release their cargo in a sustained manner [15]. For example, polymer-conjugated angiogenesis inhibitor TNP-470 (caplostatin) was found to accumulate selectively in the tumor vessels by the EPR effect and inhibit hyperpermeability of tumor blood vessels [24,25]. In studies published from our laboratory, we have shown that nanoparticle-conjugated chemotherapeutic agents such as doxorubicin [26,27] and angiogenic small molecule inhibitors [28] can preferentially home into tumors by the EPR effect, resulting in selective vascular shutdown and inhibition of tumor growth.

It should be noted that EPR alone is not always sufficient in targeting the tumor sites and hence is often used in conjunction with active targeting. This combination ensures that nanoparticles are retained in the tumor tissues following their extravasation from leaky vessels. Active targeting of tumor tissues is achieved by chemically arraying ligands on the surface of nanoparticles that can recognize and selectively bind to receptors specifically expressed on tumor cells and vessels. The high surface area to volume ratio of the nanoparticles leads to high local density of ligands for targeting. Nanoparticle-mediated active targeting of the tumor vasculature in anti-angiogenic therapy has been achieved by targeting the VEGF receptors (VEGFRs), $\alpha_v\beta_3$ integrins, and other angiogenic factors, as discussed briefly in the following section and in more details in each nanovector category later in this review.

Targeting tumor neovasculature

The most prominent modification of nanovectors entails covalently conjugating 'tags' at their surface, in order to increase their targeting potential towards tumorogenic cancer cells and/or their associated vasculature. The main 'tag' used thus far for chemotherapy involves proteins that target the integrin family. As previously mentioned, integrins are key players in the angiogenesis process, and moreover, their upregulation is known to promote survival, growth, and invasion of both tumor and endothelial cells [12]. Integrin $\alpha_v\beta_3$ has been the most widely used as a targeting moiety on nanovectors due to its pleitropic upregulation in a variety of tumor

settings [29-32], some of which have been successfully translated into several clinical trials [12,33]. However, important lacunae remain in the field, mainly owing to the inefficiency of integrin targeting in the long-run.

Nanotechnology-based approaches could remedy this limitation, due to their prolonged half-life and increased targeting efficiency. For instance, perfluorocarbon nanoparticles conjugated to various contrasting agents (Gadolinium, Gd or Fluorine isotope 19, ^{19}F) have successfully been linked to an $\alpha_v\beta_3$ integrin antibody and then visualized by magnetic resonance imaging (MRI) in rabbit and mouse models of tumor angiogenesis [29,32]. These studies open the door for non-invasive detection of various types of cancers in clinical settings, as well as for other diseases characterized by aberrant vasculature, such as atherosclerosis and other CVD [31]. In an analogous manner, another approach to target integrin overexpression consists of using a synthetic peptide containing the recognition site for integrins, namely an Arginine-Glycine-Aspartic acid (RGD) sequence [30]. Recent studies are further optimizing integrin targeting by engineering novel peptide moieties which bind with better affinity to integrins than current RGD tags [34,35].

Another characteristic of tumor-associated vasculature is inflammation, resulting in upregulation of various markers known to promote endothelial-tumor cell interactions and metastasis, such as endothelial-cell selectin (E-selectin) [36]. Although E-selectin-based nanotherapeutics have been used less extensively than integrin-targeting nanoparticles, they do provide an additional means to target activated endothelium, and might hence provide an attractive tag to be used in conjunction with integrin targeting [37].

It becomes apparent that targeting-based approaches for tumor therapies are only as good as the selectivity and specificity of the targeting moiety used. This, in turn, implies that using disease-selective markers is crucial in order to obtain maximum selectivity without deleterious side-effects. Since targeted nanotechnology is often coupled with a chemotherapeutic agent entrapped in the nanoparticle, proper targeting to the diseased tissue is crucial to minimize systemic side-effects [38]. As most diseased states are usually characterized by several markers, an attractive direction would be to combine several tags on one nanovector, so long as these do not interact with each other.

Engineering anti-angiogenic nanoparticles to suit our needs: Playing with nanovector backbone and drug coupling for therapeutic and imaging purposes

Since nanoparticles were first proposed by Marty JJ. *et al.* in 1978 as novel drug-delivery systems [39], their use as anti-cancer agents exploded during the 1980 s. However, only more recently (1995) have they been used to target angiogenesis [40]. Several nanovectors have been reported thus far in mediating anti-angiogenesis therapy and imaging of the tumor vasculature. These include an arsenal of synthetic and natural nanoparticles such as polymeric conjugates and polymeric nanoparticles; liposomes and micelles; synthetic organic nanoparticles such as dendrimers; carbon-based nanostructures such as carbon nanotubes and polyhydroxylated fullerenes; inorganic nanoparticles of gold, silver and iron-oxide; quantum dots; viral capsids and ferritin. The plethora of nanovectors allows researchers to fine-tune the properties of the drugs depending on their target. Further fine-tuning is also possible depending on the method of drug-nanovector coupling, thus offering the potential to engineer revolutionary therapeutics in the field of angiogenesis. Herein, we review the different types of nanovectors that have been studied to formulate anti-angiogenic agents for imaging and therapeutic purposes, their main modifications, as well as their advantages and limitations.

Polymeric nanoconjugates

A diverse family of polymers has been studied for the engineering of nanoparticle-based drug delivery agents since one of the earliest reports in 1979 describing their use in cancer therapy [41]. Polymers chemically conjugated to drugs are regarded as new chemical entities owing to their distinctive pharmacokinetic profile as compared to the parent drugs. Polymeric nanoparticles can also be designed to encapsulate drugs without any chemical modification. Encapsulated drugs can be control-released from the polymer matrix by diffusion or through surface or bulk erosion, while release of conjugated drugs requires cleavage of the covalent bonds under biological conditions. Some key examples of polymer-based nanoconjugates for anti-angiogenesis therapy have been prepared from structures, such as N-(2-hydroxypropyl)methacrylamide (HPMA), poly(lactic co-glycolic acid) (PLGA), polysaccharides (e.g. chitosan) and dendrimers, to name a few.

N-(2-hydroxypropyl)methacrylamide (HPMA) copolymers HPMA copolymers are hydrophilic substances that have been extensively studied for their anti-angiogenesis potential. An HPMA copolymer conjugated to the angiogenesis inhibitor TNP-470 (Caplostatin), was the first polymer-conjugated angiogenesis inhibitor reported [25]. It was found to selectively accumulate in the tumor microvasculature, resulting in decreased tumor growth rate in human melanoma and lung carcinoma mice models. Interestingly, such formulation of TNP-470 prevented it from crossing the blood-brain barrier, thus overcoming the neurotoxicity often associated with chemotherapeutic drugs. The mechanisms of actions underlying Caplostatin's chemotherapeutic effects included inhibition of various angiogenic signaling

pathways such as: VEGF receptor-2 (VEGFR-2), mitogen-activated protein kinase (MAPK) and RhoA [24]. HPMA copolymers have also been used to design novel bone-targeted anti-angiogenic therapeutic agents [42,43]. In these studies, the bone-targeting aminobisphosphonate drug alendronate (Fosamax) was co-conjugated to the polymer backbone along with a chemotherapeutic drug (e.g., paclitaxel, TNP-470), thus inhibiting bone metastasis. Here, passive targeting was achieved by extravasation of the nanoconjugates from the leaky tumor vessels via the EPR effect, while active targeting to the calcified tissues was achieved by alendronate's high affinity to the bone mineral. These studies have tremendous clinical implications, as bone metastasis is associated with a plethora of cancers, and its presence correlates with the terminal stage of cancers.

Specific peptide sequences have been conjugated to HPMA copolymers for active targeting of the $\alpha_v\beta_3$ integrin in tumor-associated vasculature. Radionuclide-labeled, cyclized RGD peptide-tagged HPMA copolymer-based nanoconjugates have been designed that provide the potential for targeted delivery of radionuclides and drugs to solid tumors for diagnostic and therapeutic applications [44,45]. The conjugates exhibited increased tumor retention times and rapid clearance from normal tissues, thus reducing systemic toxicity associated with standard therapeutics. These studies clearly demonstrated the significance of $\alpha_v\beta_3$ targeting using RGD-bearing conjugates, as this could provide a promising strategy for selective delivery of angiogenesis inhibitors and imaging agents to tumor vasculature and tumor sites expressing the $\alpha_v\beta_3$ integrin.

Poly(lactic co-glycolic acid) (PLGA) copolymers PLGA copolymers have been extensively used in the field of cancer research, owing to their biodegradability and biocompatibility, resulting in their FDA approval. PLGA is synthesized by the co-polymerization of two different monomers, lactic acid and glycolic acid, and can be further modified chemically for conjugation or simple encapsulation of drugs in a nanoparticle formulation, as shown in Figure 1. In a study targeting the MAPK signaling pathway, Basu and Harfouche *et al.* have reported the use of PLGA copolymer for chemically conjugating PD98059, a selective MAPK inhibitor [46]. The resulting nanoparticles selectively resulted in melanoma regression in a mouse model. In a consecutive study, Harfouche and Basu *et al.* encapsulated an inhibitor of the phosphatidylinositol-3-kinase (PI3K) pathway in a PLGA copolymer, and used novel zebrafish melanoma and breast adenocarcinoma tumor xenograft models to demonstrate its anti-angiogenic effect [28].

PLGA-based nanoparticles have also been used to engineer complex nanosystems. In a novel strategy reported by Sengupta *et al.*, temporal targeting of tumor

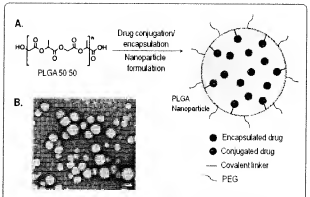

Figure 1 PLGA nanoparticles: (A) Chemical conjugation or simple encapsulation of chemotherapeutic agents in PEG-modified PLGA nanoparticles. (B) Transmission electron microscopy image of PLGA nanoparticles. Scale bar 100 nm.

cells and the tumor vasculature was achieved using a nanoscale delivery system, described as a 'nanocell', that comprised of a core PLGA nanoparticle encapsulated within a polyethylene glycol (PEG)-linked lipid envelop [26]. PEGylation of a molecule renders the latter non-toxic and non-immunogenic, and is an FDA approved method [47]. In this nanostructure, the chemotherapeutic drug doxorubicin was covalently attached to the inner PLGA core, and the anti-angiogenic agent combretastatin was trapped within the outside lipid envelope. After disruption of the outer envelope inside a tumor, release of combretastatin led to vascular collapse and intra-tumoral trapping of the nanoparticles, which subsequently released the chemotherapeutic drug in response to local hypoxia, resulting in significant regression of various tumors including melanoma. The nanocell is an example of nanoparticles being engineered based on understanding of the disease, and can be fine-tuned to optimize chemotherapy, thus shifting the paradigm from conventional anti-angiogenic treatments.

In our ongoing studies using a Zebrafish mutant, named Casper, which allows the visualization of cancer cells in real-time even when they are unlabeled [48], we demonstrated that hybrid nanoparticles of PLGA carrying an inhibitor of PI3K not only inhibited vascularization, as shown by reduced subintestinal vessel (SIV) density, but also inhibited both human melanoma and breast adenocarcinoma tumor cell growth (Figure 2).

PLGA nanoparticles have not only been used as delivery agents of synthetic drugs, but have also recently been described for delivering natural products thought to have anti-cancer effects. Curcumin (yellow pigment in the spice turmeric)-loaded PLGA nanoparticles were reported to successfully suppress tumor necrosis factor (TNF)-regulated expression of VEGF, culminating in reduced tumor metastasis [49]. This approach is promising for

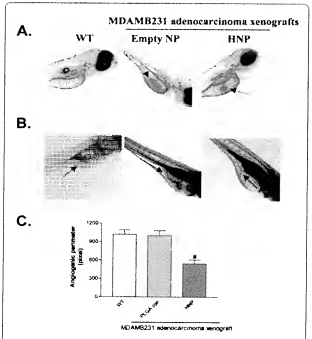

Figure 2 Effects of LY-encapsulated PLGA nanoparticles *in vivo* using Casper Zebrafish-breast adenocarcinoma xenograft assay (A) Real time imaging. Broken arrows show cancer cells. (B) Alkaline phosphatase vessel staining. Full arrows show subintestinal vessels (SIV). (C) Quantification of SIV using morphometric analyses developed in our laboratory. HNP – hybrid nanoparticles. P* ≤ 0.05 versus wild-type and empty nanoparticle controls. (in collaboration with Dr. Richard M. White and Dr. Leonard I. Zon, Children's Hospital Boston).

using natural products for chemotherapeutics, as it eliminates many side-effects observed with synthetic drugs.

Polysaccharides and Dendrimers Polysaccharides (e.g. chitosan) and dendrimers can also be considered as polymeric systems, and have been studied as carriers of anti-angiogenic agents for therapeutic applications. Chitosan is a commercially available cationic linear polysaccharide, which has found a variety of applications in pharmaceuticals and biomedicine. Dendrimers, on the other hand, possess a branched structure that provides it with certain unique properties like ease of chemical conjugation, biocompatibility, high water-solubility and easy renal clearance due to their small size [15,50]. Different dendrimeric systems are now under investigation for novel cancer treatments [50]. In a recent study, chitosan nanoparticles have shown significant inhibition of tumor growth and induction of tumor necrosis in a mouse hepatocellular carcinoma xenograft model [51]. The anti-tumor activity of these nanoparticles was found to be related with their anti-angiogenic activity, which was linked to significant reduction in the levels of VEGFR-2 expression and subsequent blockage of VEGF-induced endothelial cell activation. In using dendrimers as nanovectors, Backer *et al.* have described the construction of $VEGF_{121}$-containing, boronated polyamidoamine dendrimer that can be used to target VEGF receptors on tumor neovasculature [52]. Near-IR fluorescent imaging of mouse breast carcinoma revealed selective accumulation of these dendrimers in the periphery of growing tumors, where tumor neovascularization was most prominent. These studies demonstrate the potential of designing chitosan and dendrimer-based nanoparticles for both chemotherapeutic and imaging purposes.

Lipid-based nanoparticles

Lipid-based nanocarriers, such as liposomes and micelles, possess attractive biological properties, including biocompatibility, biodegradability, and the ability to entrap both hydrophobic and hydrophilic drugs [15]. Liposomes are FDA-approved spherical structures consisting of phospholipid bilayers with an enclosed aqueous phase that can carry a range of chemotherapeutic drugs. Micelles, on the other hand, consist of lipid monolayers with a hydrophilic shell enclosing a hydrophobic core in a spherical structure. Although liposomal nanosystems have been widely reported for anti-angiogenic therapy, reports on using micelles are relatively fewer. Benny *et al.* reported that conjugation of the angiogenesis inhibitor TNP-470 to monomethoxy-polyethyleneglycol-polylactic acid copolymer resulted in the formation of nanopolymeric micelles, named Lodamin [53]. On oral administration, the conjugate was found to accumulate selectively in tumors, inhibiting tumor growth, angiogenesis and proliferation, without causing any neurological impairment in tumor-bearing mice. In another study based on targeting the αvβ3 integrin, Nasongkla *et al.* designed a cyclic RGD pentapeptide conjugated, doxorubicin-loaded poly(ε-caprolactone)-polyethyleneglycol (PCL-PEG) nanopolymeric micelles [54]. The micelles showed high efficiency in targeting SLK tumor endothelial cells derived from human Kaposi's sarcoma *in vitro*. Since most chemotherapeutics are delivered in highly invasive manners, such as by systemic injection, this method of targeted delivery has the crucial capacity of immensely reducing discomfort and cytotoxicity in the patient.

Adding to the library of peptide-tags for targeting is a pentapeptide sequence consisting of the amino acids Alanine-Proline-Arginine-Proline-Glycine (APRPG), that has been isolated from a phage-displayed peptide library and has been found to specifically bind to tumor angiogenic vasculature [55]. APRPG-conjugated liposomal nanosystems containing chemotherapeutic drugs have been studied for their vasculature-targeting anti-angiogenic effects [56,57]. These studies demonstrated the benefits of using the APRPG-motif for active targeting of drug

carriers to angiogenic site in a novel tumor-treatment modality, namely anti-neovascular therapy [58].

Due to their ease of synthesis, liposomal systems have been used to target a plethora of angiogenic factors, including VEGFRs, αvβ3 integrins and matrix metalloproteinases (MMPs). Li *et al.* investigated the potential anti-angiogenic efficacy of two polymerized liposomal nanoparticles radiolabeled with Yttrium isotope 90 (^{90}Y), one conjugated to a small molecule integrin antagonist targeting the αvβ3 integrin and the other loaded with a monoclonal antibody against murine VEGFR-2 receptor Flk-1 [59]. Membrane type-1 matrix metalloproteinase (MT1-MMP), expressed on angiogenic endothelium cells and tumor cells, also plays an important role in angiogenesis. Hatakeyama *et al.* designed Fab' fragments of anti-human MT1-MMP monoclonal antibody conjugated to PEG-modified doxorubicin-encapsulating liposomes that showed significant decrease in tumor volume *in vivo* as compared to the non-targeted liposomes [60].

Carbon nanovectors

Carbon-based nanostructures, such as carbon nanofibers, nanotubes and fullerenes, have received considerable attention for cancer research in the past. This is due to several advantages, including: (1) high mechanical strength and surface area, (2) numerous sites for chemical or physical conjugation, (3) light weight properties, and (4) ease of scalability and manufacturing [61]. However, issues related to their biocompatibility, renal clearance and toxicology have since limited their use in biomedical applications. In addition, although an increasing number of studies have been reported on the use of carbon nanovectors in cancer research, their use in targeting angiogenesis remains limited.

Murugesan *et al.* have reported the efficacy of multi-walled carbon nanotubes, C_{60} fullerenes and graphite in inhibiting VEGF- and bFGF-induced angiogenesis in chick chorioallantoic membrane (CAM) [61]. These carbon materials did not have any significant effect on basal angiogenesis in the absence of added growth factors, indicating potential in tumor environment where angiogenic factors are known to be upregulated. In an interesting study, Chaudhuri *et al.* reported that the shape of carbon-based nanostructures markedly affects the chemotherapeutic potential of doxorubicin [27]. The authors showed differential effects between doxorubicin (Dox) conjugated to single-walled carbon nanotubes (CNT) versus spherical fullerenols (Full) on angiogenesis (Figure 3). Both empty and Dox-conjugated fullerenols exerted anti-angiogenic effects in zebrafish and mouse melanoma models. In contrast, empty and Dox-conjugated CNTs exerted a pro-angiogenic effect both *in vitro* and *in vivo*. Mechanistic studies implicated differential activation of αvβ3 integrins and downstream PI3K signaling between CNT and fullerenol in endothelial cells, which implicates the role of nanovector shapes in mediating drug fate, and

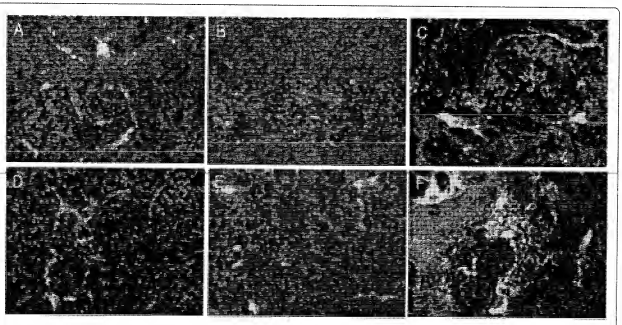

Figure 3 Effects of doxorubicin (Dox)-conjugates of fullerenols and carbon nanotubes (CNT) on B16-F10 mediated angiogenesis in mouse xenograft model. Angiogenesis was assessed by immunodetection of the Von Willebrand Factor (vWF) endothelial cell marker (green) and propidium iodide counterstain (red) on treatments with: (A) control; (B) fullerenol; (C) CNT; (D) Dox alone; (E) fullerenol-Dox conjugate; and (F) CNT-Dox conjugate.

underlies the importance of choosing the right vector to obtain optimal therapeutic index.

Inorganic nanoparticles

Inorganic nanoparticles, such as the ones derived from gold, silver and iron-oxide, possess unique optical, electrical, magnetic, and photothermal properties, which have been harnessed in numerous biomedical applications. Recently, they have been reported for use in anti-angiogenic therapy also.

Mukherjee *et al.* observed that gold nanoparticles bind specifically with heparin-binding growth factors, such as $VEGF_{165}$ and bFGF, resulting in inhibition of endothelial cell proliferation *in vitro*, and VEGF-induced permeability and angiogenesis *in vivo*, but failed to inhibit the activity of non-heparin binding growth factor $VEGF_{121}$ [62]. Gurunathan *et al.* reported on the anti-angiogenic properties of silver nanoparticles, and demonstrated that these agents could inhibit VEGF-induced cell proliferation, migration and formation of new blood microvessels *in vivo* [63]. Furthermore, their results indicated that silver nanoparticles could target the activation of PI3K/Akt signaling pathways, thus leading to the inhibitory effect of angiogenesis.

The paramagnetic properties of iron-oxide nanoparticles have been harnessed for therapeutic and imaging applications [64]. Chen *et al.* have reported that dextran-coated iron-oxide nanoparticles conjugated to radiolabeled (Iodine isotope 131, ^{131}I) anti-VEGF monoclonal antibody significantly increased imaging resolution as well as destruction of liver cancer in mice [65]. Maeng *et al.* have developed doxorubicin-loaded, folate-receptor targeted superparamagnetic iron oxide nanoparticles that significantly inhibited tumor growth, yet surprisingly, did not increase systemic cytotoxicity often associated with heavy metals, most likely due to their selective localization in tumors [66].

Imaging tumor angiogenesis

Medical imaging has undergone tremendous research and development over the past few decades, with the introduction of techniques such as magnetic resonance imaging (MRI), computed tomography (CT), ultrasonography, nuclear medicine scanning, and optical fluorescence imaging [67,68]. The possibility of non-invasive and accurate monitoring of tumor response has led to growing interest in the use of these techniques in angiogenesis research. Use of nanoparticles offer several advantages in this area of research, including their capability of carrying high payloads of therapeutic and diagnostic agents, improved contrast, and longer circulation times in the body.

MRI has been found to correlate more directly with tumor angiogenesis as compared to other imaging techniques [67]. Drevs et al. have reported the use of the dynamic enhanced MRI technique for studying the effects of PTK787/ZK 222584, a specific VEGF receptor tyrosine kinase inhibitor, on the anatomy and functional properties of tumor vessels [69]. Dextran-associated, superparamagnetic iron oxide nanoparticles (Endorem) were used in this study to detect the partial tumor blood volume in a murine renal cell carcinoma model. Reichardt et al. have also used the MRI technique and superparamagnetic nanoparticles in imaging the anti-angiogenic effects of a small molecule VEGF receptor tyrosine kinase inhibitor in a drug-resistant human adenocarcinoma model [70]. Sipkins et al. have pioneered the use of endothelial $\alpha v\beta 3$-targeted, gadolinium ion-containing paramagnetic liposomes for imaging tumor angiogenesis by MRI [71]. Intravenous administration of these nanoparticles provided detailed and enhanced imaging of the $\alpha v\beta 3$ expressing tumor vasculature in rabbit carcinomas.

A combination of two or more modalities, either in imaging or in therapeutic applications, or both, can function synergistically to provide complementary informations. A bimodal approach to imaging tumor angiogenesis, using MRI and fluorescence, was reported by Mulder et al [72]. In a following study, the same bimodal liposomal system was used for non-invasive evaluation of the therapeutic efficacy of angiogenesis inhibitors anginex and endostatin [73]. In a novel approach, Kluza et al. have functionalized a bimodal (MRI- and fluorescence-detectable) paramagnetic liposomal nanoparticle with two angiogenesis-specific targeting ligands - an $\alpha v\beta 3$-specific RGD peptide sequence and a galectin-1-specific designer peptide anginex [74]. This strategy of dual ligand targeting provided synergistic targeting effects *in vitro* significantly improving the uptake of these nanoparticles as compared to those modified for single ligand targeting.

Apart from MRI and optical imaging, liposomes have also been used to encapsulate contrast agents for CT imaging. For example, Samei et al. have reported the use of a long-circulating liposomal system encapsulating traditional iodinated contrast agent for micro-CT imaging of rats implanted with R3230AC mammary carcinoma [75].

Quantum dots (QDs), which are fluorescent nanocrystals made of inorganic semiconductor materials, have gained prominence in biomedical imaging due to their unique photostable and fluorescence properties. We observed that QD complexes, conjugated to $\alpha v\beta 3$ integrin-binding cyclic RGD peptide for endothelial cell targeting *in vitro*, showed increased uptake into the cells as compared to QDs that were conjugated to a control RAD (Arginine-Alanine-Aspartic acid) peptide (negative control) (Figure 4).

Paramagnetic QDs have been engineered as a bimodal (MRI and fluorescence) imaging probe. Such QDs

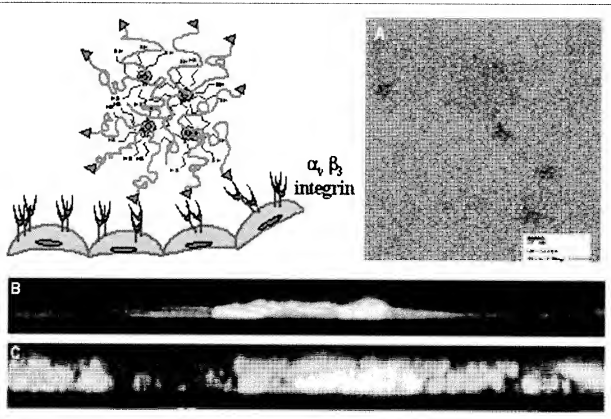

Figure 4 PEGylated Quantum Dot (QD) nanocrystals conjugated to αvβ3-specific RGD peptide for endothelial cell targeting: (A) low resolution transmission electron microscopy image showing the nanoconjugates, the arrow indicating one such nanostructure; (B and C) spinning disk confocal microscopy images showing uptake of RGD-targeted QD clusters in endothelial cells treated with cations that are known to cause integrin clustering. Incubation with the RAD-PEG-nanocrystal QD clusters showed no uptake by the cells (B), while RGD-PEG-nanocrystal QD clusters resulted in increased uptake into the cells (C).

functionalized by αvβ3-specific RGD peptide have been used for successful targeting of human endothelial cells *in vitro* [76]. In another study, paramagnetic QDs on conjugation with a cyclic peptide that can target CD13, an aminopeptidase highly overexpressed on angiogenic tumor endothelium, enabled quantitative molecular MRI of tumor angiogenesis *in vivo* [77].

Natural nanoparticles, such as viruses and ferritin, have several advantages over synthetic nanoparticles, including precise dimensions, possible evasion by the immune system, biocompatibility and biodegradability [68]. A number of viral nanoparticles (VNPs) have been developed for targeted delivery and imaging purposes, e. g. cowpea mosaic virus (CPMV) and bacteriophages such as MS2, Qβ, and their modes of cellular uptake have been studied [78]. Banerjee *et al.* have recently reported the mechanism of receptor-mediated endocytosis of transferrin-decorated bacteriophage Qβ [79]. Multivalent display of fluorescent tags on CPMV facilitated intravital visualization of human fibrosarcoma-mediated tumor angiogenesis in a CAM model [80]. In a different study, covalent attachment of a VEGF receptor-1 specific peptide to fluorescently labeled CPMV enabled efficient targeting of the VNPs to VEGFR-1-expressing tumor *in vivo* [81].

Apart from viral nanoparticles, protein cages such as the iron-containing ferritin have also been studied in medical imaging [68]. Crich et al. have reported the MRI visualization of tumor angiogenesis *in vivo* by targeting the neural cell adhesion molecules expressed on tumor endothelium with a highly sensitive gadolinium-containing apoferritin probe [82].

New generation research in anti-angiogenesis therapy

Apart from the more conventional approaches of arraying small molecule chemotherapeutic drugs or antibodies on different synthetic or natural nanovectors to achieve anti-angiogenic effects, new research reports are emerging that target the molecular mechanism of angiogenesis by using approaches such as gene silencing and

others. In the following sections, we will review some of these emerging new strategies.

Nanoconjugates for siRNA/gene delivery

An interesting strategy to target tumor vasculature is by systemic delivery of an anti-angiogenic gene using a nanoconjugate system. The soluble fragment of VEGF receptor Flt-1 (sFlt-1) is a potent and selective inhibitor of VEGF. As such, Kim *et al.* showed that the stable expression of sFlt-1 by endothelial cell targeted gene delivery inhibited angiogenesis [83]. For this purpose, the authors designed a PEGylated polyethyleneimine (PEI) nanosystem, consisting of the αvβ3 integrin targeting RGD peptide sequence, PEI-*g*-PEG-RGD, and complexed with the therapeutic gene encoding sFlt-1. The PEI-*g*-PEG-RGD/pCMV-sFlt-1 nanoconjugate system successfully inhibited the proliferation of cultured endothelial cells *in vitro* by blocking the binding of VEGF to the membrane-bound full length Flt-1 receptor. In a further study, the authors showed that this polymeric gene delivery system reduced tumor burden in mice while increasing prognosis [84].

The use of small interfering RNA (siRNA) and short-hairpin RNA (shRNA) have tremendously helped in our understanding of the molecular mechanisms underlying angiogenesis and tumor developments. The high specificity of these small RNA sequences in binding target proteins post-transcriptionally can prove crucial to our efforts in designing new generation of therapeutics [85]. In one such study, Schiffelers *et al.* have reported the engineering of RGD-sequence bearing PEGylated self-assembling polymeric nanoparticles that can be used to deliver siRNAs specifically targeted to inhibit VEGFR-2 expression, thereby inhibiting tumor angiogenesis [86]. Intravenous administration of these nanoparticles into mice bearing neuroblastoma N2A tumors led to selective tumor uptake, siRNA sequence-specific inhibition of VEGFR2 expression in tumor, and inhibition of tumor growth and angiogenesis.

Lipid-based nanosystems have also been reported for targeted gene and siRNA delivery. Protease-activated receptor-1 (PAR-1) siRNA incorporated into neutral liposomes was used to target the thrombin receptor PAR-1, which is involved in adhesion, invasion and angiogenesis [87]. Systemic delivery of these nanoparticles inhibited both melanoma tumor growth and metastasis in mice. This led to significant inhibition of tumor growth and weight, in addition to a concomitant decrease in the expression of various angiogenic factors (VEGF, interleukin-8 and MMP-2), as well as reduced blood vessel density.

Apart from polymeric and lipid-based nanosystems, chitosan nanoparticles loaded with siRNA have also been designed to provide a novel therapeutic tool for selectively knocking down angiogenesis genes. For instance, Pillé *et al.* have reported the use of a chitosan-coated poly-isohexylcyanoacrylate nanoparticle for encapsulating anti-RhoA siRNA, resulting in inhibition of tumor growth and angiogenesis in an aggressive breast cancer mouse xenograft model [88].

Aptamers

Aptamer-based nanotherapeutics have emerged as a novel strategy due to their recognition, and hence targeting, of an endless list of moieties including oncogenes, viruses, bacteria and inflammatory proteins. Aptamers are short, three-dimensional synthetic RNA or DNA oligonucleotides (15-40 nucleotides long) or peptides (10-20 amino acids long) that bind their target with high affinity and specificity, hence their nickname of 'chemical antibodies' [89-91]. Depending which epitope aptamers bind to, namely an active versus non-active site, determines whether aptamers inhibit function or simply acts as a targeting moiety. These properties make aptamers ideally suited for diagnostics, imaging and targeting of angiogenic-based pathologies. The strengths of aptamers reside in their versatility, non-immunogenicity, low cost, high reproducibility and ease of production, which become immediately apparent when compared with standards antibodies. For instance, oligonucleotide and peptide aptamers can be isolated from an impressively large repertoire of libraries, by processes known as Systematic Evolution of Ligands by Exponential Enrichment (SELEX) and yeast/bacterial expression libraries, respectively [89,91]. These libraries have been key determinants in increasing the efficacy and popularity of aptamer-based nanotechnology, as they allow high-throughput screening and can hence find disease markers. The main lacuna of aptamers are that they are easily degraded by cellular nucleases and proteinases [89]. This lacuna is easily remedied by chemical modifications of the aptamers, making them ideal candidate for novel nanotherapeutics with improved targeting power and therapeutic index [90].

Oligonucleotide aptamers have recently gained much popularity in the field of cancer in general. For instance, they have played a crucial role in increasing targeting and imaging of cancer cell and their associated vasculature by being coupled to metallic nanoparticles such as magnetic, gold and ruby-eye doped nanoparticles, as well as quantum dots [90,92-94]. This coupling of aptamers to metallic nanoparticles creates an exciting new opportunity for tumor detection, as it potentiates the biosensor capability of metallic nanoparticles significantly. Using other type of nanovectors, VEGF-targeting RNA aptamers have been combined with either PLGA microspheres or 1,2-distearoyl-*sn*-glycero-3-phosphatidylcholine (DSPC) and cholesterol nanoliposomes, resulting in potent and selective inhibition of angiogenesis *in vitro* and *in vivo* for prolonged time periods [95,96]. In another interesting

study, an Ang-2 RNA aptamer was shown to inhibit adult neovascularization in a rat corneal pocket model of tumor angiogenesis [97]. As the role of Ang-2 in mediating vascularization has long been contested, with contradicting reports demonstrating both pro- and anti-angiogenic roles, this study validates our previous findings that Ang-2 can indeed play a preponderant role in promoting angiogenesis [98].

Oligonucleotide aptamers have preferentially been used, as compared with their peptide counterparts, mainly due to their higher binding affinities and lower costs and ease of synthesis and purification. This has translated into very few reports combining peptide aptamer- and nanoparticle-based technologies, with most studies instead focusing on the advantages of these aptamers for forward and reverse genetic experiments [91]. Hence, there is currently an enormous gap with respect to peptide aptamer-based nanotherapeutics, altough the potential is certainly present, mainly due to the advantage of peptide aptamers in disrupting protein-protein interactions. As such, they have efficiently been used in cancer setting to target and inhibit various tumor markers associated with tumor growth and metastasis [99,100]. Although these latter studies didn't conjugate the aptamers with nanovectors, they open up the doors to novel and exciting possibilities in the nanotechnology field. To the best of our knowledge, peptide aptamers have only been conjugated with nanomaterials in the case of carbon, but for the sole purpose of increasing its solubility [101].

Stem cell-based nanotherapeutics

In a novel approach, embryonic stem cells have been used in conjunction with nanoparticles for either tumor imaging [102] or for pro-angiogenic therapy during CVD-related ischemia [103]. For imaging, stem cells were labeled with ferumoxides-poly-lysine complexes (e.g. iron oxide superparamagnetic nanoparticles) and used to visualize gliomas using MRI. This finding has enormous therapeutic implications, since very few agents are able to bypass the blood brain barrier, often resulting in insurmountable obstacles for the treatment of brain malignancies. Regarding pro-angiogenic stem cell-based therapeutics, cells were transfected with VEGF DNA using biodegradable poly(β-amino esters) nanoparticles, leading to significant vascular regeneration in ischemic tissues [103]. This methodology in itself is quite novel, as standard transfection methods rely on plasmids or electroporation, which results in high cell stress and low efficiency. Although there are very few studies merging nanotechnology with stem cells, this field warrants further investigation due to its immense clinical potential in a variety of angiogenic diseases, especially those characterized by vessel insufficiency. In a novel approach, our laboratory has attempted to merge the use of carbon nanovectors with embryonic stem cells. Our preliminary results show that the shape of carbon nanostructures can modulate stem cell fate, with an example of an inhibitory effect on vascularization, as shown in Figure 5. Our ongoing studies underlie the infinite possibilities of

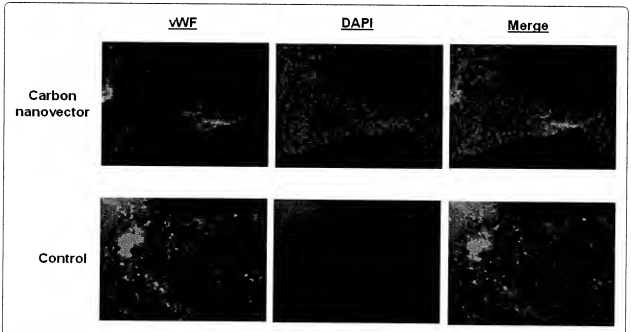

Figure 5 Carbon nanovectors inhibit stem cell-mediated vascularization Immunocytochemistry results show Von Willebrand Factor (vWF) endothelial cell marker (red) and DAPI counterstain (blue).

modulating tissue regeneration with, not only scaffold type, but structure as well.

Concluding Remarks and Future Directions

The tumor neovasculature is an attractive target for anti-angiogenic therapy as well as non-invasive imaging studies. Nanotechnology has emerged as an exciting field in this area of research due to multiple advantages, including the capacity of nanoparticles to carry multiple moities of therapeutic and imaging agents, offer longer circulation time and increase the therapeutic index of chemotherapeutcs, to name a few. Moreover, with the various types of nanovectors available, many of which are FDA-approved, along with the various methods for coupling them to drugs and diagnostic agents, there is an endless opportunity to fine-tune nanotherapeutics depending on the task needed. Clearly, the advent of nanothechnology provides a huge potential for devising increasingly novel anti-angiogenic therapeutics that can eventually be translated from bench to bed-side.

Acknowledgements

The authors would like to thank Dr. Richard M. White and Dr. Leonard I. Zon (Children's Hospital Boston) for providing Casper Zebrafish and for their advice, as well as Dr. Dirk M. Hentschel and Dr. Joseph V. Bonventre (Harvard Institutes of Medicine, Boston, MA) for access to Zebrafish facilities. This work was funded by a CIHR fellowship to Parisa Haffouche, and a Department of Defense BCRP Era of Hope Scholar Award (W81XWH-07-1-0482) and a BCRP Innovator Collaborative Award, and a NIH RO1 (1R01CA135242-01A2) to Shiladitya Sengupta.

Authors' contributions

DB and RH collected the references and compiled the manuscript. DB, RH and SS edited the manuscript. All authors read and approved the final manuscript.

Competing interests

The authors declare that they have no competing interests.

Received: 23 August 2010 Accepted: 31 January 2011
Published: 31 January 2011

References

1. Weidner N, Semple JP, Welch WR, Folkman J: Tumor angiogenesis and metastasis– correlation in invasive breast carcinoma. *N Engl J Med* 1991, 324:1-8
2. Risau W: Mechanisms of angiogenesis. *Nature* 1997, 386:671-674
3. Folkman J: Angiogenesis in cancer, vascular, rheumatoid and other disease. *Nat Med* 1995, 1:27-31.
4. Folkman J: Tumor angiogenesis: therapeutic implications. *N Engl J Med* 1971, 285:1182-1186
5. Naumov GN, Akslen LA, Folkman J: Role of angiogenesis in human tumor dormancy: animal models of the angiogenic switch. *Cell Cycle* 2006, 5:1779-1787
6. Chaplain MA: Mathematical modelling of angiogenesis. *J Neuroncol* 2000, 50:37-51
7. Folkman J: Incipient angiogenesis 1. *J Natl Cancer Inst* 2000, 92:94-95
8. Weidner N, Folkman J, Pozza F, Bevilacqua P, Allred EN, Moore DH, Meli S, Gasparini G: Tumor angiogenesis: a new significant and independent prognostic indicator in early-stage breast carcinoma 1. *J Natl Cancer Inst* 1992, 84:1875-1887
9. Fukumura D, Jain RK: Imaging angiogenesis and the microenvironment. *APMIS* 2008, 116:695-715
10. Boudreau N, Myers C: Breast cancer-induced angiogenesis: multiple mechanisms and the role of the microenvironment. *Breast Cancer Res* 2003, 5:140-146
11. Khadaroo RN, Yu J, Tabaye E, Darga T, Brown CK, Mauceri HJ, Yassari R, Gupta N, Weichselbaum RR: Tumour-endothelium interactions in co-culture: coordinated changes of gene expression profiles and phenotypic properties of endothelial cells. *J Cell Sci* 2003, 116:1017-1027.
12. Desgrosellier JS, Cheresh DA: Integrins in cancer: biological implications and therapeutic opportunities. *Nat Rev Cancer* 2010, 10:9-22.
13. Yeh CH, Peng HC, Huang TF: Accutin, a new disintegrin, inhibits angiogenesis in vitro and in vivo by acting as integrin alphavbeta3 antagonist and inducing apoptosis. *Blood* 1998, 92:3268-3276
14. Liekens S, De Clercq E, Neyts J: Angiogenesis: regulators and clinical applications. *Biochem Pharmacol* 2001, 61:253-270.
15. Peer D, Karp JM, Hong S, Farokhzad OC, Margalit R, Langer R: Nanocarriers as an emerging platform for cancer therapy. *Nat Nanotechnol* 2007, 2:751-760.
16. Ferrara N: VEGF as a therapeutic target in cancer. *Oncology* 2005, 69(Suppl 3):11-16.
17. Folkman J: Fundamental concepts of the angiogenic process. *Curr Mol Med* 2003, 3:643-651
18. Segal E, Satchi-Fainaro R: Design and development of polymer conjugates as anti-angiogenic agents. *Adv Drug Deliv Rev* 2009, 61:1159-1176.
19. Kerbel RS, Kamen BA: The anti-angiogenic basis of metronomic chemotherapy. *Nat Rev Cancer* 2004, 4:423-436.
20. Davis ME, Chen ZG, Shin DM: Nanoparticle therapeutics: an emerging treatment modality for cancer. *Nat Rev Drug Discov* 2008, 7:771-782
21. Sun SS, Fenniri H, Singh B: Nanotechnology-based drug delivery systems. *J Occup Med Toxicol* 2007, 2:16.
22. Farokhzad OC, Langer R: Impact of nanotechnology on drug delivery. *ACS Nano* 2009, 3:16-20.
23. Couvreur P, Vauthier C: Nanotechnology: intelligent design to treat complex disease. *Pharm Res* 2006, 23:1417-1450.
24. Satchi-Fainaro R, Mamluk R, Wang L, Short SM, Nagy JA, Feng D, Dvorak AM, Dvorak HF, Puder M, Mukhopadhyay D, Folkman J: Inhibition of vessel permeability by TNP-470 and its polymer conjugate, caplostatin. *Cancer Cell* 2005, 7:251-261.
25. Satchi-Fainaro R, Puder M, Davies JW, Tran HT, Sampson DA, Greene AK, Corfas G, Folkman J: Targeting angiogenesis with a conjugate of HPMA copolymer and TNP-470. *Nat Med* 2004, 10:255-261.
26. Sengupta S, Eavarone D, Capila I, Zhao G, Watson N, Kiziltepe T, Sasisekharan R: Temporal targeting of tumour cells and neovasculature with a nanoscale delivery system. *Nature* 2005, 436:568-572.
27. Chaudhuri P, Harfouche R, Soni S, Hentschel DM, Sengupta S: Shape effect of carbon nanovectors on angiogenesis. *ACS Nano* 2010, 4:584-592.
28. Harfouche R, Basu S, Soni S, Hentschel DM, Mashelkar RA, Sengupta S: Nanoparticle-mediated targeting of phosphatidylinositol-3-kinase signaling inhibits angiogenesis. *Angiogenesis* 2009.
29. Anderson SA, Rader RK, Westlin WF, Null C, Jackson D, Lanza GM, Wickline SA, Kotyk JJ: Magnetic resonance contrast enhancement of neovasculature with alpha(v)beta(3)-targeted nanoparticles. *Magn Reson Med* 2000, 44:433-439.
30. Park JH, Kwon S, Nam JO, Park RW, Chung H, Seo SB, Kim IS, Kwon IC, Jeong SY: Self-assembled nanoparticles based on glycol chitosan bearing 5beta-cholanic acid for RGD peptide delivery. *J Control Release* 2004, 95:579-588.
31. Winter PM, Morawski AM, Caruthers SD, Fuhrhop RW, Zhang H, Williams TA, Allen JS, Lacy EK, Robertson JD, Lanza GM, Wickline SA: Molecular imaging of angiogenesis in early-stage atherosclerosis with alpha(v)beta3-integrin-targeted nanoparticles. *Circulation* 2003, 108:2270-2274
32. Waters EA, Chen J, Yang X, Zhang H, Neumann R, Santeford A, Arbeit JM, Lanza GM, Wickline SA: Detection of targeted perfluorocarbon nanoparticle binding using 19F diffusion weighted MR spectroscopy. *Magn Reson Med* 2008, 60:1232-1236.
33. Rong L, Habuchi H, Kimata K, Lansdall LJ, Kusche-Gullberg M: Substrate specificity of the heparan sulfate hexuronic acid 2-O-sulfotransferase. *Biochemistry* 2001, 40:5548-5555.
34. Xie J, Shen Z, Li KC, Danthi N: Tumor angiogenic endothelial cell targeting by a novel integrin-targeted nanoparticle. *Int J Nanomedicine* 2007, 2:479-485.

35. Buehler A, van Zandvoort MA, Stelt SJ, Hackeng TM, Schiens-Stassen BH, Bennaghmouch A, Hofstra L, Creutzberg JP, Daemen JH, Duijvestijn A, Smeets MB, de Kleijn DP, Post MJ, de Munnck ED: **cNGR: a novel homing sequence for CD13/APN targeted molecular imaging of murine cardiac angiogenesis in vivo.** *Arterioscler Thromb Vasc Biol* 2006, **26**:2681-2687.
36. Hebbar M, Peyrat JP: **Significance of soluble endothelial molecule E-selectin in patients with breast cancer.** *Int J Biol Markers* 2000, **15**:15-21.
37. Kang HW, Josephson L, Petrovsky A, Weissleder R, Bogdanov A Jr: **Magnetic resonance imaging of inducible E-selectin expression in human endothelial cell culture.** *Bioconjug Chem* 2002, **13**:122-127.
38. Wagner S, Rothweiler F, Anhorn MG, Sauer B, Riemann I, Weiss FC, Katsen-Globa A, Michaelis M, Cinatl J, Schwartz D, Kreuter J, von BH, Langer K: **Enhanced drug targeting by attachment of an anti alpha v integrin antibody to doxorubicin loaded human serum albumin nanoparticles.** *Biomaterials* 2010, **31**:7388-7396.
39. Marty JJ, Oppenheim RC, Speiser P: **Nanoparticles--a new colloidal drug delivery system.** *Pharm Acta Helv* 1978, **53**:17-23.
40. Winet H, Hollinger JO, Stevanovic M: **Incorporation of polylactide-polyglycolide in a cortical defect: neoangiogenesis and blood supply in a bone chamber.** *J Cranio Pro* 1995, **13**:679-689.
41. Couvreur P, Kante B, Roland M, Speiser P: **Adsorption of antineoplastic drugs to polyalkylcyanoacrylate nanoparticles and their release in calf serum.** *J Pharm Sci* 1979, **68**:1521-1524.
42. Segal L, Pan H, Ofek P, Udagawa T, Kopeckova P, Kopecek J, Satchi-Fainaro R: **Targeting angiogenesis-dependent calcified neoplasms using combined polymer therapeutics.** *PLoS ONE* 2009, **4**:e5233.
43. Miller K, Erez R, Segal E, Shabat D, Satchi-Fainaro R: **Targeting bone metastases with a bispecific anticancer and antiangiogenic polymer-alendronate-taxane conjugate.** *Angew Chem Int Ed Engl* 2009, **48**:2949-2954.
44. Mitra A, Mulholland J, Nan A, McNeill E, Ghandehari H, Line BR: **Targeting tumor angiogenic vasculature using polymer-RGD conjugates.** *J Control Release* 2005, **102**:191-201.
45. Mitra A, Coleman T, Borgman M, Nan A, Ghandehari H, Line BR: **Polymeric conjugates of mono- and bi-cyclic alphaVbeta3 binding peptides for tumor targeting.** *J Control Release* 2006, **114**:175-183.
46. Basu S, Harfouche R, Soni S, Chimote G, Mashelkar RA, Sengupta S: **Nanoparticle-mediated targeting of MAPK signaling predisposes tumor to chemotherapy.** *Proc Natl Acad Sci USA* 2009, **106**:7957-7961.
47. Veronese FM, Pasut G: **PEGylation, successful approach to drug delivery.** *Drug Discov Today* 2005, **10**:1451-1458.
48. White RM, Sessa A, Burke C, Bowman T, LeBlanc J, Ceol C, Bourque C, Dovey M, Goessling W, Burns CE, Zon LI: **Transparent adult zebrafish as a tool for in vivo transplantation analysis.** *Cell Stem Cell* 2008, **2**:183-189.
49. Anand P, Nair HB, Sung B, Kunnumakkara AB, Yadav VR, Tekmal RR, Aggarwal BB: **Design of curcumin-loaded PLGA nanoparticles formulation with enhanced cellular uptake, and increased bioactivity in vitro and superior bioavailability in vivo.** *Biochem Pharmacol* 2010, **79**:330-338.
50. Gillies ER, Frechet JM: **Dendrimers and dendritic polymers in drug delivery.** *Drug Discov Today* 2005, **10**:35-43.
51. Xu Y, Wen Z, Xu Z: **Chitosan nanoparticles inhibit the growth of human hepatocellular carcinoma xenografts through an antiangiogenic mechanism.** *Anticancer Res* 2009, **29**:103-109.
52. Backer MV, Gaynutdinov TI, Patel V, Bandyopadhyaya AK, Thirumamagal BT, Tjarks W, Barth RF, Claffey K, Backer JM: **Vascular endothelial growth factor selectively targets boronated dendrimers to tumor vasculature.** *Mol Cancer Ther* 2005, **4**:1423-1429.
53. Benny O, Lamarca G, Adini A, Cassiola F, Bazinet L, Adini I, Pravda E, Nahmias Y, Koirala S, Corfas G, D'Amato RJ, Folkman J: **An orally delivered small-molecule formulation with antiangiogenic and anticancer activity.** *Nat Biotechnol* 2008, **26**:799-807.
54. Nasongkla N, Shuai X, Ai H, Weinberg BD, Pink J, Boothman DA, Gao J: **cRGD-functionalized polymer micelles for targeted doxorubicin delivery.** *Angew Chem Int Ed Engl* 2004, **43**:6323-6327.
55. Oku N, Asai T, Watanabe K, Kuromi K, Nagatsuka M, Kurohane K, Kikkawa H, Ogino K, Tanaka M, Ishikawa D, Tsukada H, Momose M, Nakayama J, Taki T: **Anti-neovascular therapy using novel peptides homing to angiogenic vessels.** *Oncogene* 2002, **21**:2662-2669.
56. Asai T, Shimizu K, Kondo M, Kuromi K, Watanabe K, Ogino K, Taki T, Shuto S, Matsuda A, Oku N: **Anti-neovascular therapy by liposomal DPP-CNDAC targeted to angiogenic vessels.** *FEBS Lett* 2002, **520**:167-170.
57. Maeda N, Takeuchi Y, Takada M, Sadzuka Y, Namba Y, Oku N: **Anti-neovascular therapy by use of tumor neovascularture-targeted long-circulating liposome.** *J Control Release* 2004, **100**:41-52.
58. Shimizu K, Asai T, Oku N: **Antineovascular therapy, a novel antiangiogenic approach.** *Expert Opin Ther Targets* 2005, **9**:63-76.
59. Li L, Wartchow CA, Danthi SN, Shen Z, Dechene N, Pease J, Choi HK, Doede T, Chu P, Ning S, Lee DY, Bednarski MD, Knox SJ: **A novel antiangiogenesis therapy using an integrin antagonist or anti-Flk-1 antibody coated 90Y-labeled nanoparticles.** *Int J Radiat Oncol Biol Phys* 2004, **58**:1271-1277.
60. Hatakeyama H, Akita H, Ishida E, Hashimoto K, Kobayashi H, Aoki T, Yasuda J, Obata K, Kikuchi H, Ishida T, Kiwada H, Harashima H: **Tumor targeting of doxorubicin by anti-MT1-MMP antibody-modified PEG liposomes.** *Int J Pharm* 2007, **342**:196-205.
61. Murugesan S, Mousa SA, Ostermeier U, Lincoln DW, Linhardt RJ: **Carbon inhibits vascular endothelial growth factor-and fibroblast growth factor-promoted angiogenesis.** *FEBS Lett* 2007, **581**:1157-1160.
62. Mukherjee P, Bhattacharya R, Wang P, Wang L, Basu S, Nagy JA, Atala A, Mukhopadhyay D, Soker S: **Antiangiogenic properties of gold nanoparticles.** *Clin Cancer Res* 2005, **11**:3530-3534.
63. Gurunathan S, Lee KJ, Kalishwaralal K, Sheikpranbabu S, Vaidyanathan R, Eom SH: **Antiangiogenic properties of silver nanoparticles.** *Biomaterials* 2009, **30**:6341-6350.
64. McCarthy JR, Kelly KA, Sun EY, Weissleder R: **Targeted delivery of multifunctional magnetic nanoparticles.** *Nanomedicine (Lond)* 2007, **2**:153-167.
65. Chen J, Wu H, Han D, Xie C: **Using anti-VEGF McAb and magnetic nanoparticles as double-targeting vector for the radioimmunotherapy of liver cancer.** *Cancer Lett* 2006, **231**:169-175.
66. Maeng JH, Lee DH, Jung KH, Bae YH, Park IS, Jeong S, Jeon YS, Shim CK, Kim W, Kim J, Lee J, Lee YM, Kim JH, Kim W-S, Hong SS: **Multifunctional doxorubicin loaded superparamagnetic iron oxide nanoparticles for chemotherapy and magnetic resonance imaging in liver cancer.** *Biomaterials* 2010, **31**:4995-5006.
67. Cristofanilli M, Charnsangavej C, Hortobagyi GN: **Angiogenesis modulation in cancer research: novel clinical approaches.** *Nat Rev Drug Discov* 2002, **1**:415-426.
68. Cormode DP, Jarzyna PA, Mulder WJ, Fayad ZA: **Modified natural nanoparticles as contrast agents for medical imaging.** *Adv Drug Deliv Rev* 2010, **62**:329-338.
69. Drews J, Muller-Driver R, Wittig C, Fuxius S, Esser N, Hunjenschmidt H, Kuzendorf MA, Allegrini PR, Wood J, Hennig J, Unger C, Marme D: **PTK787/ZK 222584, a specific vascular endothelial growth factor-receptor tyrosine kinase inhibitor, affects the anatomy of the tumor vascular bed and the functional vascular properties as detected by dynamic enhanced magnetic resonance imaging.** *Cancer Res* 2002, **62**:4015-4022.
70. Reichardt W, Hui-Lowe D, Torres D, Weissleder R, Bogdanov A Jr: **Imaging of VEGF receptor kinase inhibitor-induced antiangiogenic effects in drug-resistant human adenocarcinoma model.** *Neoplasia* 2005, **7**:847-853.
71. Sipkins DA, Cheresh DA, Kazemi MR, Nevin LM, Bednarski MD, Li KC: **Detection of tumor angiogenesis in vivo by alphaVbeta3-targeted magnetic resonance imaging.** *Nat Med* 1998, **4**:623-626.
72. Mulder WJ, Strijkers G, Habets JW, Bleeker EJ, van der Schaft DW, Storm G, Koning GA, Griffioen AW, Nicolay K: **MR molecular imaging and fluorescence microscopy for identification of activated tumor endothelium using a bimodal lipidic nanoparticle.** *FASEB J* 2005, **19**:2008-2010.
73. Mulder WJ, van der Schaft DW, Hautvast PA, Strijkers GJ, Koning GA, Storm G, Mayo KH, Griffioen AW, Nicolay K: **Early in vivo assessment of angiostatic therapy efficacy by molecular MRI.** *FASEB J* 2007, **21**:378-383.
74. Mura E, van der Schaft DW, Hautvast PA, Mulder WJ, Mayo KH, Griffioen AW, Strijkers GJ, Nicolay K: **Synergistic targeting of alphavbeta3 integrin and galectin-1 with heteromultivalent paramagnetic liposomes for combined MR imaging and treatment of angiogenesis.** *Nano Lett* 2010, **10**:52-58.
75. Samee E, Saunders RS, Badea CT, Ghaghada KB, Hedlund LW, Qi Y, Yuan H, Bentley RC, Mukundan S Jr: **Micro-CT imaging of breast tumors in rodents using a liposomal, nanoparticle contrast agent.** *Int J Nanomedicine* 2009, **4**:277-282.
76. Mulder WJ, Koole R, Brandwijk RJ, Storm G, Chin PT, Strijkers GJ, de Mello DC, Nicolay K, Griffioen AW: **Quantum dots with a paramagnetic coating as a bimodal molecular imaging probe.** *Nano Lett* 2006, **6**:1-6.

77. Oostendorp M, Douma K, Hackeng TM, Dirksen A, Post MJ, van Zandvoort MA, Backes WH: Quantitative molecular magnetic resonance imaging of tumor angiogenesis using cNGR-labeled paramagnetic quantum dots. *Cancer Res* 2008, **68**:7676-7683.
78. Manchester M, Singh P: Virus-based nanoparticles (VNPs): platform technologies for diagnostic imaging. *Adv Drug Deliv Rev* 2006, **58**:1505-1522.
79. Banerjee D, Liu AF, Voss NR, Schmid SL, Finn MG: Multivalent display and receptor-mediated endocytosis of transferrin on virus-like particles. *Chemosichem* 2010, **11**:173-1279.
80. Lewis JD, Destito G, Zijlstra A, Gonzalez MJ, Quigley JP, Manchester M, Stuhlmann H: Viral nanoparticles as tools for intravital vascular imaging. *Nat Med* 2006, **12**:354-360.
81. Brunel FM, Lewis JD, Destito G, Steinmetz NF, Manchester M, Stuhlmann H, Dawson PE: Hydrazone ligation strategy to assemble multifunctional viral nanoparticles for cell imaging and tumor targeting. *Nano Lett* 2010, **10**:1093-1097.
82. Geninatti CS, Bussolati B, Tei L, Grange C, Esposito G, Lanzardo S, Camussi G, Aime S: Magnetic resonance visualization of tumor angiogenesis by targeting neural cell adhesion molecules with the highly sensitive gadofolinium-loaded apoferritin probe. *Cancer Res* 2006, **66**:9196-9201.
83. Kim WJ, Yockman JW, Lee M, Jeong JH, Kim YH, Kim SW: Soluble Flt-1 gene delivery using PEI-g-PEG-RGD conjugate for anti-angiogenesis. *J Control Release* 2005, **106**:228-234.
84. Kim WJ, Yockman JW, Jeong JH, Christensen LV, Lee M, Kim YH, Kim SW: Anti-angiogenic inhibition of tumor growth by systemic delivery of PEI-g-PEG-RGD/pCMV-sFlt-1 complexes in tumor-bearing mice. *J Control Release* 2006, **114**:361-368.
85. Hadj-Slimane R, Lepelletier Y, Lopez N, Garbay C, Raynaud F: Short interfering RNA (siRNA), a novel therapeutic tool acting on angiogenesis. *Biochime* 2007, **89**:1234-1244.
86. Schiffelers RM, Ansari A, Xu J, Zhou Q, Tang Q, Storm G, Molema G, Lu FY, Scaria PV, Woodle MC: Cancer siRNA therapy by tumor selective delivery with ligand-targeted sterically stabilized nanoparticle. *Nucleic Acids Res* 2004, **32**:e149.
87. Villares GJ, Zigler M, Wang H, Melnikova VO, Wu H, Friedman R, Leslie MC, Vivas-Mejia PE, Lopez-Berestein G, Sood AK, Bar-Eli M: Targeting melanoma growth and metastasis with systemic delivery of liposome-incorporated protease-activated receptor-1 small interfering RNA. *Cancer Res* 2008, **68**:9078-9086.
88. Pille JY, Li H, Blot E, Bertaux JR, Pritchard LL, Opolon P, Maksimenko A, Lu H, Vannier JP, Soria J, Malvy C, Soria C: Intravenous delivery of anti-RhoA small interfering RNA loaded in nanoparticles of chitosan in mice: safety and efficacy in xenografted aggressive breast cancer. *Hum Gene Ther* 2006, **17**:1019-1026.
89. Kvasi M: The future of aptamers in medicine. *J Clin Pathol* 2010.
90. Lee JH, Yigit MV, Mazumdar D, Lu Y: Molecular diagnostic and drug delivery agents based on aptamer-nanomaterial conjugates. *Adv Drug Deliv Rev* 2010.
91. Crawford M, Woodman R, Ko FP: Peptide aptamers: tools for biology and drug discovery. *Brief Funct Genomic Proteomic* 2003, **2**:72-79.
92. Wang W, Chen C, Qian M, Zhao XS: Aptamer biosensor for protein detection using gold nanoparticles. *Anal Biochem* 2008, **373**:213-219.
93. Esteves MC, Huang YF, Kang H, O'Donoghue MB, Bamrungsap S, Yan J, Chen X, Tan W: Nanoparticle-aptamer conjugates for cancer cell targeting and detection. *Methods Mol Biol* 2010, **624**:235-248.
94. Smith JE, Medley CD, Tang Z, Shangguan D, Lofton C, Tan W: Aptamer-conjugated nanoparticles for the collection and detection of multiple cancer cells. *Anal Chem* 2007, **79**:3075-3082.
95. Carrasquillo KG, Ricker JA, Rigas IK, Miller JW, Gragoudas ES, Adamis AP: Controlled delivery of the anti-VEGF aptamer EYE001 with poly(lactic-co-glycolic)acid microspheres. *Invest Ophthalmol Vis Sci* 2003, **44**:290-299.
96. Mills MC, Collins BO, Zhang T, Green LS, Sebesta DP, Bell C, Kellogg E, Gill SC, Magallanez A, Knauer S, Bendele RA, Gill PS, Janjic N: Liposome-anchored vascular endothelial growth factor aptamers. *Bioconjug Chem* 1998, **9**:573-582.
97. White RR, Shan S, Rusconi CP, Shetty G, Dewhirst MW, Kontos CD, Sullenger BA: Inhibition of rat corneal angiogenesis by a nuclease-resistant RNA aptamer specific for angiopoietin-2. *Proc Natl Acad Sci USA* 2003, **100**:5028-5033.
98. Harfouche R, Hussain SN: Signaling and regulation of endothelial cell survival by angiopoietin-2. *Am J Physiol Heart Circ Physiol* 2006, **291**:H1655-H1645.
99. Merin DA, Hoppe-Seyler K, Hoppe-Seyler F, Hassaan J, Burwinkel B: Targeting Id1 and Id3 by a specific peptide aptamer induces E-box promoter activity, cell cycle arrest, and apoptosis in breast cancer cells. *Breast Cancer Res Treat* 2010.
100. Zhao RM, Hoffmann FM: Inhibition of transforming growth factor-beta1-induced signaling and epithelial-to-mesenchymal transition by the Smad-binding peptide aptamer Trx-SARA. *Mol Biol Cell* 2006, **17**:3819-3831.
101. Matsumura S, Sato S, Yudasaka M, Iomida A, Tsuruo T, Iijima S, Shiba K: Prevention of carbon nanohorn agglomeration using a conjugate composed of comb-shaped polyethylene glycol and a peptide aptamer. *Mol Pharm* 2009, **6**:441-447.
102. Anderson SA, Glod J, Arbab AS, Noel M, Ashari P, Fine HA, Frank JA: Noninvasive MR imaging of magnetically labeled stem cells to directly identify neovasculature in a glioma model. *Blood* 2005, **105**:420-425.
103. Yang E, Cho SW, Son SM, Bogatyrev SR, Singh D, Green JJ, Mei Y, Park S, Bhang SH, Kim BS, Langer R, Anderson DG: Genetic engineering of human stem cells for enhanced angiogenesis using biodegradable polymeric nanoparticles. *Proc Natl Acad Sci USA* 2010, **107**:3317-3322.

doi:10.1186/2045-824X-3-3
Cite this article as: Banerjee *et al.*: Nanotechnology-mediated targeting of tumor angiogenesis. *Vascular Cell* 2011, **3**:3.

EXHIBIT B

Gastrointestinal Uptake of Biodegradable Microparticles: Effect of Particle Size

Manisha P. Desai,[1,2] Vinod Labhasetwar,[1,2] Gordon L. Amidon,[2] and Robert J. Levy[1,2,3]

Received July 8, 1996; accepted September 9, 1996

Purpose. To investigate the effect of microparticle size on gastrointestinal tissue uptake.

Methods. Biodegradable microparticles of various sizes using polylactic polyglycolic acid (50:50) co-polymer (100 nm, 500 nm, 1 μm, and 10 μm) and boving serum albumin as a model protein were formulated by water-in-oil-in-water emulsion solvent evaporation technique. The uptake of microparticles was studied in rat *in situ* intestinal loop model and quantitatively analyzed for efficiency of uptake.

Results. In general, the efficiency of uptake of 100 nm size particles by the intestinal tissue was 15–250 fold higher compared to larger size microparticles. The efficiency of uptake was dependent on the type of tissue, such as Peyer's patch and non patch as well as on the location of the tissue collected i.e. duodenum or ileum. Depending on the size of microparticles, the Peyer's patch tissue had 2–200 fold higher uptake of particles than the non-patch tissue collected from the same region of the intestine. Histological evaluation of the tissue sections demonstrated that 100 nm particles were diffused throughout the submucosal layers while the larger size nano/microparticles were predominantly localized in the epithelial lining of the tissue.

Conclusions. There is a microparticle size dependent exclusion phenomena in the gastrointestinal mucosal tissue with 100 nm size particles showing significantly greater tissue uptake. This has important implications in designing of nanoparticle-based oral drug delivery systems, such as an oral vaccine system.

KEY WORDS: oral; drug delivery; nanoparticles; Peyer's patches; size exclusion; vaccine.

INTRODUCTION

Biodegradable particulate carrier systems are of interest as a potential means for oral delivery to enhance drug absorption (1–4), improve bioavailability (5), targeting of therapeutic agents to particular organ and reduce toxicity (6,7), to improve gastric tolerance of the agents irritant to the stomach (8) and as a carrier for antigen in oral immunization (9). The Gut Associated Lymphoid Tissue (GALT), such as lamina propria, intraepithelial lymphocytes, isolated lymphoid follicles, and Peyer's patches are the primary immune system of the gastrointestinal tract (10,11). Orally administered particulate matters gain entry into the follicle associated epithelium overlying the dome region of Peyer's patches, via M cells (12–15). Several studies have demonstrated the uptake of orally administered polystyrene particles by the Peyer's patch tissue and their subsequent translocation to discrete anatomical compartments, such as the mesenteric lymph vessels, lymph nodes, and in lesser amounts in the liver and the spleen (16–18) which could trigger both mucosal and systemic immune responses. Microparticles, in addition to protecting antigen from gastric pH and proteolytic enzymes also act as an adjuvant because they produce an elevated immune response compared to soluble antigen (9,19–21).

Several studies have been carried out with various types of polymeric materials to investigate the factors influencing the gastrointestinal uptake of microparticles (18,22–24). Size of the microparticles in studies by Jani et al. using polystyrene particles has shown to have influence on efficiency of uptake (18). Following oral gavage, the extent of absorption of particles smaller than 100 nm was significantly higher than larger size particles with more than 60% of the total uptake from the Peyer's patches of the small intestine (18,25). Thus by using optimal size microparticles as a carrier system for antigen, the immune response could be improved. Therefore, our objective in this study is to investigate the efficacy of uptake of various size biodegradable PLGA microparticles, containing BSA as a model antigen, by the gastrointestinal tissue. The goals in this study are to: (i) formulate and characterize microparticles of 100 nm, 500 nm, 1 μm and 10 μm diameter, (ii) evaluate uptake of various size microparticles in *in situ* rat intestinal loop model, and (iii) study histological localization of various size microparticles following *in situ* experiment.

MATERIALS

Polylactic polyglycolic acid copolymer (PLGA, 50 : 50, MW-100,000, inherent viscosity: 1.07 measured in hexafluoroisopropanol) was obtained from Birmingham polymers Inc., AL. Other chemicals used were polyvinyl alcohol (PVA, MW: 30,000–70,000) and bovine serum albumin (BSA, Fraction V) obtained from Sigma Chemical Co. (St. Louis, MO); 6-coumarin from Polyscience Inc., (Warrington, PA) and sodium salt of 1-heptane sulfonic acid from Aldrich Chemical Co., (Milwaukee, WI). Methylene chloride, chloroform, acetonitrile, ethyl acetate were of either HPLC grade or of an American Chemical Society Reagent grade.

Animals

Male Sprague Dawley adult rats (200–250 g wt., 12–15 weeks old) were obtained from the reproductive services at the University of Michigan. Experiments were carried out in compliance with the regulations of University Committee on Use and Care of Animals (UCUCA) at the University of Michigan.

METHODOLOGY

Formulation of PLGA Nanoparticles and Microparticles

Microparticles of various sizes of an average diameter of 100 nm, 500 nm, 1 μm and 10 μm were formulated by optimizing formulation parameters as shown in Table I. In brief, an aqueous BSA solution (10% w/v) was emulsified in a polymer solution (3–15% w/v PLGA) in methylene chloride, using a microtip probe sonicator set at 65 watts of energy output (Miso-

[1] University of Michigan, Division of Pediatric Cardiology, Ann Arbor, Michigan 48109.

[2] University of Michigan, College of Pharmacy, Ann Arbor, Michigan 48109.

[3] To whom correspondence should be addressed.

0724-8741/96/1200-1838$09.50/0

Table I. Formulation and BSA Loading of Different Size Microparticles

PLGA Solution (w/v %)	PVA Solution (w/v %)	Emulsion (w/o/w)	Desired Diameter	Actual Diameter mean ± s.e.m. n = 50	BSA Loading, (wt %) mean ± s. e. m. n = 3	Encapsulation Efficiency, (%) mean ± s. e. m. n = 3
3.0	2.5	Sonicator	100 nm	116.0 ± 5.0 nm	7.82 ± 0.23	31.28 ± 0.9
15.0	0.5	Microfluidizer	500 nm	528.0 ± 20.0 nm	4.92 ± 0.03	19.69 ± 0.1
6.0	0.5	Homogenizer	1 μm	1.1 ± 0.1 μm	4.47 ± 0.53	17.89 ± 2.1
3.0	2.5	Vortex	10 μm	9.4 ± 0.2 μm	5.48 ± 0.04	21.80 ± 0.2

nix Inc. Model XL 2020™, Farmingdale, NY) for 10 min. over an ice bath to form a water-in-oil (w/o) emulsion. The polymer solution also contained 0.05% w/v 6-coumarin as a fluorescent marker. The o/w emulsion was further emulsified into an aqueous PVA solution (0.5–2.5% w/v) to form a water-in-oil-in-water (w/o/w) emulsion.

The w/o/w emulsion was stirred over a magnetic stir plate overnight at room temperature to evaporate methylene chloride. Particles of 100 nm were recovered by ultracentrifugation (Beckman model XL-70, Arlington Hts., IL) at 100,000 g for 20 minutes. Larger size microparticles were recovered by centrifugation at 3000 rpm for 20 minutes (Ice Centra-7R, International Equipment Co., Needham Hts, MA). The particles were washed three times with water to remove PVA and unencapsulated BSA, and resuspended in water prior to lyophilization.

Characterization of Microparticles

Particle Size Distribution

Particles of 100 nm diameter were characterized for size distribution using a dynamic laser defractometer (NICOMP, Model 370, Hiac/Royco Instruments Division, Santa Barbara, CA). Optical microscopy (Olympus CHT-001, Olympus Corporation, Lake Success, NY) was used to measure the size distribution and diameter of other size particles. In addition, scanning electron microscopy (SEM) was performed to determine the surface topography of the particles. A sample of microparticles was placed on a double stick tape over aluminum stubs to get an uniform layer of particles. Sample was gold coated using a sputter gold coater (Denton Vacuum Inc., Cherry Hill, NJ) at 40 milliampere current and 50 millitorr pressure for 200 seconds at the thickness of 300 A°. Gold coated particle samples were cooled over dry ice prior to SEM observations to avoid their melting under high magnification due to the electron beam exposure (Hitachi S570, Cherry Hill, NJ).

BSA Loading of Microparticles

In a typical procedure, a sample of microparticles (5–10 mg) dissolved in 5 ml chloroform was extracted five times with each extract of 5 ml water. The combined aqueous extracts was assayed for BSA content using the coomassie blue micro BioRad® (BIO-RAD Laboratories, Hercules, CA) protein assay.

SDS-Polyacrylamide Gel Electrophoresis (SDS-PAGE)

BSA extracted from microparticles as described above was lyophilized and analyzed by SDS- PAGE to see changes, if any, in BSA following it's encapsulation into microparticles. Samples were mixed with 1.5 M Tris-HCl buffer (pH 6.8) containing 10% SDS, 40% glycerol, 0.02% bromophenol blue and 5% 2-mercaptoethanol, were heated at 95°C for 5 min. and subjected to electrophoresis at 40 mA in a vertical slab Mini-PROTEAN® II gel (BIO-RAD Laboratories, Hercules, CA). Proteins were visualized by silver staining in water, methanol and acetic acid (30 : 50 : 10 by volume).

In Vitro Release of BSA from Microparticles

The *in vitro* release of BSA from PLGA microparticles was carried out under physiologic condition at 37°C. A sample of microparticles (5 mg) suspended in 5 ml phosphate buffer (pH 7.4) was placed in the donor chamber of the double diffusion cells, separated by a 0.1 μm Millipore® (Type VV, Bedford, MA) membrane. The buffer in the receiver chamber was replaced periodically with fresh buffer. The samples were assayed for the BSA levels using micro BioRad® protein assay.

In Vitro Release of 6-Coumarin from Nanoparticles

A suspension of 100 nm particles (4 mg/ml) in PBS was placed on a rotary shaker at 37°C for two hours. Periodic samples were subjected to centrifugation at 10,000 g and the supernatant was analyzed for the released 6-coumarin by HPLC assay as described later.

Acute Animal Model Studies

Uptake of Microparticles in Rat In Situ *Intestinal Tissue Loop Model*

Animals were fasted with free access to water for 18–24 hours prior to the experiments. Rats were given general anesthesia with an intraperitoneal injection of sodium pentobarbital (6.5 mg/100 g body weight). A midline abdominal incision exposed the small intestine. Two separate intestinal segments (duodenal and ileal) of 15–20 cm length were created by incising approximate length of small bowel, that were then clamp sealed with a Kelly clamp. These segments of intestine were infused with about 100 ml of normal saline to wash off the intestinal food contents and were ligated with 2.0 Ethicon sutures (Ethicon Inc., Somerville, NJ) to form two loops, one in the region of duodenum and other in the region of ileum (26).

An aliquot of the microparticle suspension (4 mg/ml) in normal saline was infused into these segments using a syringe. After two hours, the loops were opened, microparticle suspension was drained out from each loop and the segments were

flushed with 100 ml normal saline. Loops were isolated and cut open through the mid-line incision. Mucin was scraped off with a metal spatula from the inner lining of intestine to remove the adsorbed particles. The Peyer's patch and the non-patch tissue were isolated from the intestine using a 4 mm diameter Baker's biopsy punch (Cummins Dermatologicals Inc., Miami, FL). The tissue samples were immersed in normal saline for an hour to wash off the residual mucin layer (24). Each tissue sample was blotted gently, weighed, and frozen until taken for further analysis. The length of the intestinal segment into which the microparticle suspension was infused was measured to determine the total amount of microparticles infused into each segment.

In a separate study, a control experiment was carried out by infusing a 6-coumarin solution (0.51 μg/ml) into the rat intestinal loops under identical conditions as those used for the microparticle infusion experiment described above. This is the amount of 6-coumarin that is released from the 100 nm particles in two hours under *in vitro* physiologic conditions at a 4 mg/ml nanoparticle concentration. The control experiment was carried out to ensure that the 6-coumarin estimated in the tissue was associated with the microparticles taken up by the tissue and not due to the uptake of 6-coumarin that is released from the microparticles during two hours of experimental period. The amount of 6-coumarin in each of the tissue samples was quantitated by HPLC as described below.

Animal Model Retrieval Analysis

Extraction of 6-Coumarin from Tissue Samples

Each tissue sample was homogenized separately with 1 ml of double distilled water using a high speed homogenizer (Stir-Pak®, Lab mixer, Cole-Parmer Instruments Co., Chicago, IL) for about 15 minutes over an ice-bath. The homogenate was extracted five times with 3 ml ethyl acetate at each extraction step. The combined extracts from each tissue sample were evaporated using a SpeedVac evaporator (SpeedVac® Plus SC110A, Savant Instruments, Inc., Farmingdale, NY). The residue was reconstituted with 200 μl acetonitrile for HPLC analysis.

HPLC Assay for 6-Coumarin

The Waters (Milford, MA) HPLC system consisted of a pump (model 501), an autosampler (Wisp model 712), a data module (model 740), and a μBondapak C_{18} column with 10 μm packing. Separations were achieved using acetonitrile : water : 1-heptane sulfonic acid sodium salt (50 : 50 : 0.005 M) as a mobile phase. The eluents were monitored using a scanning fluorescence detector (model 470,) at 450 nm excitation wavelength and 490 nm emission wavelength.

For each batch of microparticles, a standard curve for 6-coumarin was constructed by spiking different weight concentrations of microparticles (10 μg to 80 μg) followed by extraction of 6-coumarin and analysis by HPLC as discussed above. The amount of microparticles (μg) taken up by each tissue sample was calculated from the standard curve for corresponding size of microparticles.

The number of particles taken up by the Peyer's patch and the non patch tissue was estimated from the weight of microparticles taken up by the tissue using the following equation (27):

$$\text{Number of particles} = \frac{w \times k \times 10^9}{d^3} \quad (1)$$

where, w is the mass of particle uptake in μg per sq. mm area of the tissue, d is the diameter of particles in μm, and k is the factor (1.426) that takes into account the density (gm/cc) of the polymer used.

The Efficiency of Particle Uptake in the Rat In Situ Model

The total surface area of the intestinal loop in the *in situ* experiment that was used to infuse the microparticles was calculated from the length and diameter. From the total area of the intestinal loop as calculated above and the total amount of microparticles infused, a theoretical dose of microparticles per unit area of the intestine exposed was calculated (μm/mm²). The estimated dose calculated as above was 6.5 μg microparticles per sq. mm area of intestinal tissue exposed. The efficiency of uptake of microparticles for each particle size was determined from the actual uptake of microparticles ('w' in μg/mm²) and the estimated dose of the microparticles as calculated above.

Histology

Tissue samples were embedded in a cryostat medium (OTC, TEK II 4583, Miles Inc., Elkhart, IN) and snap frozen in isopentane and then in liquid nitrogen. Tissue sections of 7 μm thickness were cut using a microtome cryostat (Model CTI, International Equipment Company, Needham Hts., MA) at −18 to −20°C. The sections were fixed on glass slides by warming for 30 seconds. The sections were mounted in a drop of Vectashield® (Vector Labs, Inc., Burlingame, CA) and were viewed under a fluorescence microscope (Model Orthoplan, Leitz, W. Germany) using a FITC filter (wavelength 450–490 nm).

Statistical Methods

Results are presented as mean ± s.e.m. Statistical comparisons were made with students t-test at a 99% confidence level. Difference between the tissue uptake of microparticles was considered statistically significant at $p < 0.01$.

RESULTS

Formulation and Characterization of Various Size Microparticles

Microparticles of the desired particle size were obtained by optimizing various formulation parameters and energy source input used to form the w/o/w emulsions. As can be seen from the SEM analysis, all four sizes of particles formulated were spherical with smooth uniform surfaces (Fig. 1) with more than 80% particles in the desired size range. In general, BSA loading was in the range of 4% to 8% w/w with encapsulation efficiency in the range of 15% to 32%. This variation in BSA loading is due to differences in the composition and the emulsification protocol used.

In this study, all size nano/microparticles demonstrated *in vitro* an initial burst release of 10% to 20% of the encapsulated

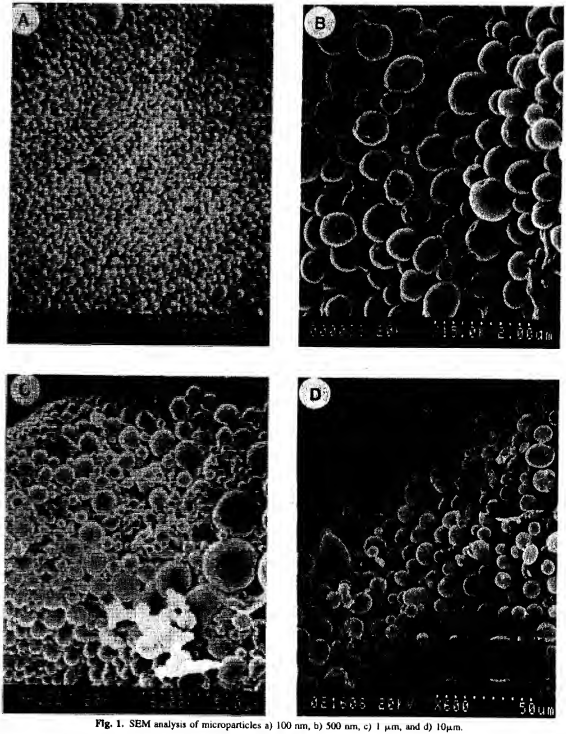

Fig. 1. SEM analysis of microparticles a) 100 nm, b) 500 nm, c) 1 µm, and d) 10µm.

BSA within first two days. The subsequent release of BSA up to 20 days was at a slower releasing rate during which only an additional 10% to 20% of the BSA was released. This slow release phase was followed by a second burst release from day 20–60 possibly due to hydrolytic erosion of the polymer matrix (Fig. 2). The difference in the burst effect for various size microparticles seems to be due to variation in the formulation composition and conditions. SDS-PAGE analysis of the encap-

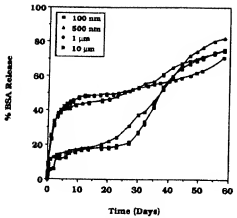

Fig. 2. *In Vitro* release of bovine serum albumin from various size PLGA microparticles (n = 3).

sulated protein shows bands that correlated with intact BSA indicating that the protein does not interact chemically with the matrix material into PLGA microparticles or does not lead to a significant irreversible aggregation of the protein.

In Situ Uptake of Microparticles

The microparticle uptake by the Peyer's patch tissue was significantly higher ($p < 0.001$) for 100 nm particles compared to all other sizes of particles (Fig. 3). In addition, the Peyer's patch tissue appears to have comparatively higher uptake of particles than nonpatch tissue. Furthermore, the Peyer's patch and the nonpatch tissue from the ileum had comparatively higher uptake of microparticles than the identical tissues collected from the region of duodenum ($p < 0.001$).

For each particle size range, the uptake of microparticles was calculated in terms of their number from the diameter, the weight of the microparticles taken up by the tissue, and the density of the PLGA polymer as per equation (i). Nanoparticles of 100 nm diameter were found to be present at levels which were several folds higher in number compared to larger size particles. For example, the number of the 100 nm particles per sq. mm of Peyer's patch is 4×10^6 fold higher than 10 μm size microparticles and 6.7×10^3 fold higher than 1 μm particles (Table II). The tissue 6-coumarin levels in the group infused with nanoparticle were several fold higher than the tissue coumarin levels detected in the control experiment, indicating that 6-coumarin levels detected in the tissue were mainly due to the coumarin contained within the particles (Fig. 4).

Histological Evaluation of Microparticle Uptake

Histological examination of the Peyer's patch and the non patch samples showed a higher level of uptake for the 100 nm particles compared to larger size particles. Particles of 100 nm diameter were seen diffused throughout the submucosal layer as well as on the serosal side of the Peyer's patch. Microparticles of 500 nm, 1 μm and 10 μm sizes were taken up to a much lesser extent and were mainly seen localized in the epithelial lining of the Peyer's patch and the nonpatch microvilli (Fig. 5A–J).

DISCUSSION

The efficiency of uptake of microparticle encapsulated antigen by the gastrointestinal lymphoidal tissue is a key factor in the successful development of an oral vaccine system. Our studies demonstrated that the 100 nm size particles have a significantly higher efficiency of uptake by the intestinal tissue in terms of their total mass and the number compared to larger size particles. Thus, it implies that the total mass of the antigen uptake by the tissue encapsulated in the smaller size nanoparticles will be significantly higher. Histological examination of the Peyer's patch and the non-patch tissue shows that nanoparticles were distributed into the submucosal layers as compared to larger size particles which were mostly aligned at the epithelial linings. Thus it seems that there is a particle size dependent exclusion phenomena with smaller size particles more likely to be internalized inside the cells and tissue. This has significant importance in the development of a successful oral vaccine system because oral immunization results in poor immune

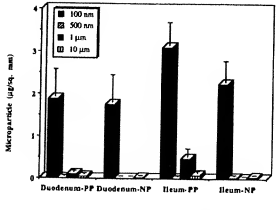

Fig. 3. *In situ* uptake of microparticles by rat intestinal tissue in weight (μg) of particles per sq. mm area of rat intestinal tissue. PP = Peyer's patch and NP = non-patch tissue (n = 15–20).

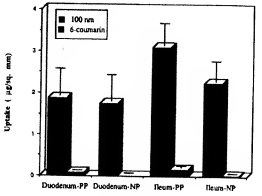

Fig. 4. Comparative *in situ* uptake of 100 nm particles and 6-coumarin from Peyer's patch and non-patch tissue; $p < 0.001$ (n = 10).

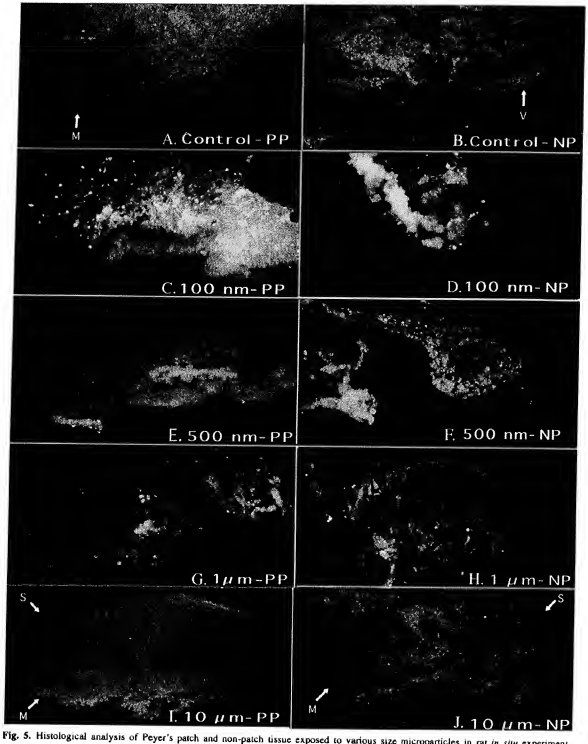

Fig. 5. Histological analysis of Peyer's patch and non-patch tissue exposed to various size microparticles in rat *in situ* experiment. PP = Peyer's patch and NP = non patch tissue, M = mucosa, S = serosa and V = villi.

response mainly due to very low efficiency of uptake of an orally administrated antigen.

In other studies, investigators have used particles in micron size range and demonstrated that PLGA (85:15) particles >5 μm in diameter cannot traverse in the Peyer's patch and are not seen systemically (28). Similar studies (not using nanoparticles) by Ebel (24) showed greater uptake of <5 μm fluorescent polystyrene latex particles in the Peyer's patch in mice. It is

Table II. Microparticle Uptake in Number/mm^2 and % Efficiency of Uptake from Rat Intestinal Tissue[a]

Particle Size[b]	Microparticle (Number/mm^2):[% Efficiency, mean ± s.e.m.]			
	Duodenum-PP	Ileum-PP	Duodenum-NP	Ileum-NP
100 nm	2.7×10^5 [30.07 ± 10.30]	4.4×10^5 [49.57 ± 8.34]	2.5×10^5 [27.88 ± 10.30]	3.2×10^5 [35.69 ± 7.85]
500 nm	8.4×10^4 [0.12 ± 0.06]	7.9×10^4 [0.11 ± 0.06]	4.4×10^4 [0.06 ± 0.02]	1.9×10^5 [0.27 ± 0.12]
1 μm	1.3×10^5 [1.51 ± 0.51]	6.5×10^5 [7.45 ± 3.05]	5.9×10^2 [0.01 ± 0.01]	1.3×10^3 [0.01 ± 0.01]
10 μm	0.7×10^2 [0.80 ± 0.19]	1.2×10^2 [1.33 ± 0.70]	0.2×10^2 [0.26 ± 0.07]	0.4×10^2 [0.48 ± 0.11]

Note: Dose = 6.25 μm/mm^2; n = 15 − 23 samples. PP = Peyer's Patch; NP = Non Patch Tissue.
[a] $p < 0.001$; 116 nm particles vs. 519 nm, 1 μm and 9.4 μm particles.
[b] Nominal Sizes; Actual mean diameters were 116 nm, 519 nm, 1 μm and 9.4 μm.

also hypothesized by Florence et al. (14) that nanoparticles because of their smaller size would also have an efficient disposition via Peyer's patches to other lymphatic organs such as to the mesenteric lymph nodes and to spleen to induce systemic immune response.

Smaller size nanoparticles could also have efficient gastrointestinal tissue uptake by other routes, such as uptake by intracellular pathways. Nanoparticles could gain entry in the tissue through intracellular spaces and especially in larger defects of the mucosa. Several other investigators too noticed this phenomena with smaller size particles (29,30). In a morphological study, Sanders and Ashworth (16) found that 200 nm latex particles were taken up into jejunal absorptive cells of adult rats. The particles were observed in intact intracellular vesicles and were then discharged into the lamina propria.

Although there is no proposed reeeptor based mechanism for the uptake of particulate matter by the M cells, particles may be taken up by a non specific endocytosis. Several physical properties of microparticles could influence their interactions within the M cells and also other cells of the gastrointestinal tissue. Other investigators have also demonstrated that hydrophobic microparticles have higher efficiency of uptake compared to hydrophilic particles (28). Thus it seems that apart from particle size and hydrophobicity, factors such as surface charge and other interfacial and surface properties of microparticles could also influence their uptake by the gastrointestinal tissue. Jani and co-workers have demonstrated that uptake of non-ionized polystyrene nanoparticles was greater than the uptake of negatively charged (carboxylated) particles by the rat gastrointestinal tissue after oral gavage (17).

Thus, nanoparticles could prove to have potential applications in oral drug delivery including vaccine in oral immunization due to their efficient uptake by the GALT, and also to improve oral bioavailability of therapeutic agents (5). In addition, oral administration of nanoparticles encapsulated agent could provide sustained drug effect because these can become trapped in the microvilli, thus prolonging their gastrointestinal transit time. The slow breakdown of the polymer would provide sustained release of therapeutic agent over a period of time. An enteric coated capsule or time release capsule could be used to deliver these nanoparticles, bypassing gastric pH. Although the efficiency of uptake of 100 nm particles observed in this study is under optimally controlled experimental conditions, *in vivo* it could be influenced by several other factors such as the presence of food, interaction of nanoparticles with luminal contents and contact of nanoparticles with gastrointestinal tissue, however the size exclusion dependent phenomenon will remain consistent with the findings of this study.

CONCLUSIONS

i. This study demonstrated that 100 nm size nanoparticles show significantly greater uptake than larger size nano/microparticles.

ii. The increased uptake of smaller particles could broaden the uses for nanoparticle delivery systems to include intestinal administration of vaccines, proteins and peptides (such as insulin) and DNA for transgene delivery.

iii. The increased uptake of smaller particles by GALT implies that smaller nanoparticles may be particularly well suited for use with vaccines.

ACKNOWLEDGMENTS

This work was partially supported by TSRL Inc., Ann Arbor, MI, under a subcontract from the U.S. Army SBIR program (V. L.) (Contract # DAMD17-95-C-5060), and by the Matrigen Corporation (R. J. L.), Ann Arbor, MI. Authors thank Ardith Bates for her secretarial assistance.

REFERENCES

1. P. Couvreur, B. Kante, M. Roland and P. Speiser. *J. Pharm. Sci.* **68 (12)**:1521–1524 (1979).
2. P. Couvreur, V. Lenaerts, D. Leyh, P. Guiot and M. Roland. In Microspheres and Drug Therapy. Pharmaceuticals, Immunological and Medical Aspects. Edited by S. S. Davis, L. Illum, J. G. McVie and E. Tomlinson., Elsevier Science Publishers B. V. 103–115 (1984).
3. J. Kreuter. *Inter. J. Pharm.* **14**:43–58 (1983).
4. L. Illum, S. S. Davis, R. H. Muller, E. Mak and P. West. *Life Sci.* **40**:367–374 (1987).
5. P. Maincent, R. Le Verge, P. A. Sado, P. Couvreur and J. P. Devissaguet. *J. Pharm. Sci.* **75**:955–958 (1986).
6. P. A. Kramer and T. Burnstein. *Life Sci.* **19**:515–520 (1976).
7. J. J. Marty, R. C. Oppenheim and P. P. Speiser. *Pharm. Acta Helv.* **53**:17–23 (1978).
8. C. M. Adeyeye, J. D. Bricker, V. D. Vilivalam and W. I. Smith. *Pharm. Res.* **13**:784–793 (1996).
9. J. Mestecky, Z. Moldoveanu, M. Novak, W. Q. Huang, R. M. Gilley, J. K. Staas, D. Schafer and R. W. Compans. *J. Control. Rel.* **28**:131–141 (1994).
10. C. A. Gilligan and A. L. Wan Po. *Inter. J. Pharm.* **75**:1–24 (1991).
11. D. T. O'Hagan, K. J. Palin and S. S. Davis. *CRC Critical Reviews in Therapeutic Drug Carrier Systems.* **4**:197–220 (1987).
12. H. O. Alpar, W. N. Field, R. Hyde and D. A. Lewis, *J. Pharm. Pharmacol.* **41**:194–196 (1989).

13. M. E. LeFevre, J. W. Vanderhoff, J. A. Laissue and D. D. Joel. *Experientia.*. **34**:120–122 (1978).
14. A. T. Florence and P. U. Jani. In Pharmaceutical Particulate Carriers. Therapeutic Application. Edited by Alain Rolland, Marcel Dekker Inc. **61**:65–108 (1993).
15. J. Pappo and T. H. Ermak. *Clin. Exp. Immunol.* **76**:144–148 (1989).
16. E. Sanders and C. T. Ashworth. *Exp. Cell Res.* **22**:137–145 (1961).
17. P. Jani, G. W. Halbert, J. Langridge and A. T. Florence. *J. Pharm. Pharmacol.* **41**:809–812 (1989).
18. P. Jani, G. W. Halbert, J. Langridge and A. T. Florence. *J. Pharm. Pharmacol.* **42**:821–826 (1990).
19. D. S. Cox and M. A. Taubman. *Int. Archs Allergy Appl. Immun.* **75**:126–131 (1984).
20. O. Strannegard and A. Yurchision. *Int. Arch. Allergy.* **35**:579–590 (1969).
21. J. R. McGhee, J. Mestecky, M. T. Dertzbaugh, J. H. Eldridge, M. Hirasawa and H. Kiyono. *Vaccine* **10**:75–88 (1992).
22. M. E. LeFevre and D. D. Joel. In Intestinal Toxicology. Edited by C. M. Schiller. Raven Press. 45–56 (1984).
23. J. H. Eldridge, J. K. Staas, J. A. Meulbroek, J. R. McGhee, T. R. Tice and R. M. Gilley. *Mol. Immunol.* **28**:287–294 (1991).
24. J. P. Ebel. *Pharm. Res.* **7**:848–451 (1990).
25. A. M. Hillery, P. U. Jani and A. T. Florence. *J. Drug Targetting.* **2**:151–156 (1994).
26. H. Tomizawa, Y. Aramaki, Y. Fujii, T. Hara, N. Suzuki, K. Yachi, H. Kikuchi and S. Tsuchiya. *Pharm. Res.* **10**:549–552 (1993).
27. R. H. Muller. In Colloidal carriers for controlled drug delivery and targeting. *CRC Press, Boston.* 43–45 (1991).
28. J. H. Eldridge, C. J. Hammond, J. A. Muelbroek, J. K. Staas, R. M. Gilley and T. R. Tice. *J. Control. Rel.* **11**:205–214 (1990).
29. C. Damge, C. Michel, M. Aprahamian, P. Couvreur and J. P. Devissaguet. *J. Control. Rel.* **13**:233–237 (1990).
30. M. Aprahamian, C. Michel, W. Humbert, J. P. Devissaguet and C. Damge. *Bio. Cell.* **61**:69–74 (1987).